ESC European Society of Cardiology

European Heart Journal - Cardiovascular Imaging (2025) **00**, 1–29
https://doi.org/10.1093/ehjci/jeaf014

EACVI DOCUMENT

The role of multi-modality imaging for the assessment of left atrium and left atrial appendage: a clinical consensus statement of the European Association of Cardiovascular Imaging (EACVI), European Heart Rhythm Association (EHRA) of the European Society of Cardiology (ESC)

Leyla Elif Sade [1,2]*, Francesco Fluvio Faletra[3], Gianluca Pontone[4,5], Bernhard Lothar Marie Gerber[6], Denisa Muraru [7,8], Thor Edvardsen [9,10], Bernard Cosyns[11], Bogdan A. Popescu[12], Allan Klein [13], Thomas H. Marwick[14], Matteo Cameli[15], Muhamed Saric[16], Liza Thomas [17,18,19], Nina Ajmone Marsan [20], Ricardo Fontes-Carvalho[21,22], Tomaz Podlesnikar[23,24], Marianna Fontana[25], Andre La Gerche[26], Steffen Erhard Petersen[27,28], Sarah Moharem-Elgamal[29], Marcio Sommer Bittencourt[1,2], Mani A. Vannan[30], Michael Glikson[31], Petr Peichl [32], Hubert Cochet[33], Ivan Stankovic [34], and Erwan Donal [35]

This document was reviewed by members of the 2022–24 EACVI Scientific Documents Committee, Philippe Bertrand, Yohann Bohbot, Maja Cikes, Marc Dweck, Julia Grapsa, Niall Keenan, and Valtteri Uusitalo, and by reviewers from EHRA, Deneke Thomas and de Riva Silva Marta

[1]Department of Medicine, University of Pittsburgh, School of Medicine, Pittsburgh, PA, USA; [2]Department of Cardiology, University of Pittsburgh Medical Center, Heart and Vascular Institute, Pittsburgh, PA, USA; [3]University of Pittsburgh Medical Center, Department of Cardiology, ISMETT-IRCCS, Palermo, Italy; [4]Department of Perioperative Cardiology and Cardiovascular Imaging, Centro Cardiologico Monzino IRCCS, Milan, Italy; [5]Department of Biomedical, Surgical and Dental Sciences, University of Milan, Milan, Italy; [6]Department of Cardiovascular Diseases and CARD Unit, Cliniques Universitaires Saint-Luc, Institut de Recherche Expérimentale et Clinique (IREC), Université Catholique de Louvain, Brussels, Belgium; [7]Department of Medicine and Surgery, University of Milano-Bicocca, Milan, Italy; [8]Department of Cardiology, Instituto Auxologico Italiano, IRCCS, Milan, Italy; [9]Department of Cardiology, Oslo University Hospital Rikshospitalet, Oslo, Norway; [10]Faculty of Medicine, Institute of Clinical Medicine, University of Oslo, Oslo, Norway; [11]Department of Cardiology, Centrum voor Hart- en Vaatziekten (CHVZ), Vrije Universiteit Brussel (VUB), Universitair Ziekenhuis Brussel (UZ Brussel), Brussels, Belgium; [12]Emergency Institute for Cardiovascular Diseases 'Prof. Dr. C.C. Iliescu', University of Medicine and Pharmacy 'Carol Davila'—Euroecolab, Bucharest, Romania; [13]Center for the Diagnosis and Treatment of Pericardial Diseases, Section of Cardiovascular Imaging, Department of Cardiovascular Medicine, Heart, Vascular and Thoracic Institute, Cleveland Clinic, Cleveland, OH, USA; [14]Baker Heart and Diabetes Institute, Melbourne, Victoria 3004, Australia; [15]Department of Medical Biotechnologies, Division of Cardiology, University of Siena, Siena, Italy; [16]Leon H. Charney Division of Cardiology, New York University, Langone Health, New York, NY, USA; [17]Department of Cardiology, Westmead Hospital, Sydney, Australia; [18]Westmead Clinical School, University of Sydney, Australia; [19]Southwest Clinical School, University of New South Wales, Sydney, Australia; [20]Department of Cardiology, Leiden University Medical Center, Albinusdreef 2, 2300RC Leiden, The Netherlands; [21]Departamento de Cardiologia—Unidade Local de Saúde Gaia e Espinho, Vila Nova de Gaia, Portugal; [22]RISE-Health, Departamento de Cirurgia e Fisiologia, Faculdade de Medicina, Universidade do Porto, Porto, Portugal; [23]Department of Cardiac Surgery, University Medical Centre Maribor, Maribor, Slovenia; [24]Department of Cardiology, University Medical Centre Ljubljana, Ljubljana, Slovenia; [25]Center for Amyloidosis, Division of Medicine, National Amyloidosis Centre, Royal Free Hospital UK, University College London, UK; [26]HEART Lab, St Vincent's Institute, Fitzroy, VIC, Sidney, Australia; [27]William Harvey Research Institute, NIHR Barts Biomedical Research Centre, Queen Mary University London, Charterhouse Square, London, UK; [28]Barts Heart Centre, St Bartholomew's Hospital, Barts Health NHS Trust, London, UK; [29]Adult Congenital Heart Disease Centre, Liverpool Heart and Chest Hospital, Liverpool L14 3PE, UK; [30]Marcus Heart Valve Center, Piedmont Heart Institute, Atlanta, USA; [31]Jesselson Integrated Heart Center, Shaare Zedek Medical Center Eisenberg R&D authority, Hebrew University Faculty of Medicine, Jerusalem, Israel; [32]Department of Cardiology, Institute for Clinical and Experimental Medicine, Prague, Czech Republic; [33]Department of Cardiovascular Imaging, University of Bordeaux, CHU Bordeaux, IHU LIRYC—INSERM 1045, Bordeaux, France; [34]Department of Cardiology, Clinical Hospital Centre Zemun, Faculty of Medicine, University of Belgrade, Belgrade, Serbia; and [35]Department of Cardiology, University of Rennes, CHU Rennes, Inserm, LTSI -UMR 1099, Rennes, France

Received 25 December 2024; accepted 30 December 2024; online publish-ahead-of-print 15 January 2025

* Corresponding author. E-mail: sadele2@upmc.edu

Structural, architectural, contractile, or electrophysiological alterations may occur in the left atrium (LA). The concept of LA cardiopathy is supported by accumulating scientific evidence demonstrating that LA remodelling has become a cornerstone diagnostic and prognostic marker. The structure and the function of the LA and left atrial appendage (LAA), which is an integral part of the LA, are key elements for a better understanding of multiple clinical conditions, most notably atrial fibrillation, cardioembolism, heart failure, and mitral valve diseases. Rational use of various imaging modalities is key to obtain the relevant clinical information. Accordingly, this clinical consensus document from the European Association of Cardiovascular Imaging, in collaboration with the European Heart Rhythm Association, provides comprehensive, up-to-date, and evidence-based guidance to cardiologists and cardiac imagers for the best practice of imaging LA and LAA for the diagnosis, management, and prognostication of the patients.

Keywords left atrium • left atrial appendage • imaging • atrial fibrillation • stroke • anticoagulation • echocardiography • cardiac magnetic resonance • cardiac computerized tomography • cardiomyopathy

Introduction

Structural, architectural, contractile, or electrophysiological alterations may occur in the left atrium (LA).[1] The concept of LA cardiopathy is supported by accumulating scientific evidence demonstrating that LA remodelling has become a cornerstone diagnostic and prognostic marker. The structure and the function of the LA and left atrial appendage (LAA), which is an integral part of the LA, are key elements for a better understanding of multiple clinical conditions, most notably atrial fibrillation (AF), cardioembolism, heart failure (HF), and mitral valve diseases. Rational use of various imaging modalities is key to obtain the relevant clinical information. Accordingly, this clinical consensus document aims to elucidate the state-of-the-art, disease-centred multi-modality imaging of LA and LAA to provide practical advice for the diagnosis, management, and prognostication of the patients. Intraprocedural guidance, technical aspects of the procedures, or the indications of interventions related to LA and LAA are out of the scope of this document. The clinical advice is based on evidence and/or consensus of the writing group and is classified into several categories, as shown in *Advice table 1*. Advice aims to encourage optimal use of imaging for the benefit of the patients.

Advice table 1 Categories of clinical advice

Strength of advice definition	Symbol
Clinical advice, based on robust evidence	
Clinical advice, based on uniform consensus of the writing group	
May be appropriate, based on published evidence	
May be appropriate, based on consensus within the writing group	
Area of uncertainty	

Morphology and function of LA and LAA

Normal morphology and function

LA consists of the main body and LAA. The main body of the LA consists of three components without clear anatomic demarcations: (i) the venous inflow component that receives blood from pulmonary veins (PVs); (ii) the vestibule, the outlet part surrounding the mitral orifice; and (iii) the inter-atrial septum (IAS).[2] Smooth endocardium lines the thin muscular walls of the LA body which can be described as superior (the roof), posterior, left lateral, septal (or medial), and anterior. Normal LA function has three phases: (i) PV forward flow (reservoir phase) during ventricular systole, (ii) PV forward flow during early diastole (conduit phase), and (iii) PV reverse flow by LA contraction during late diastole (absent in AF)[3] (*Figures 1* and *2*).

PVs enter the LA from the posterosuperior wall with frequent anatomic variations. Typically, two PVs (upper, lower) from each lung enter the LA with a funnel-shaped orifice which makes it difficult to see the clear demarcation of the ostium. An accessory right PV and common trunk of upper and lower PVs at entry are common variations (see CCT).

The LAA is a finger-like extension of the anterolateral LA wall located in the left atrioventricular groove, with a well-defined, usually oval orifice (the ostium), a neck region, and a lobulated body. Based on the shape of the central and secondary lobes, LAA morphology can be classified into four types with possible overlaps: windsock (single central lobe), chicken wing (bended central lobe), cauliflower (short central lobe and several lobes leading to a distal width larger than the proximal part), and cactus (central lobe leading to several secondary lobes superior and inferiorly).[3,4] The inner surface of the LAA is lined by the pectinate muscles with prominent indentations.

Remodelling and abnormal function of LA and LAA

The relationship between LV function and LA volume is complex and dynamic. Various factors such as volume and pressure overload in the context of mitral stenosis (MS), regurgitation, left ventricular (LV) systolic and/or diastolic dysfunction (DD), or AF contribute to the remodelling and dilatation of the LA. LA enlargement frequently occurs along the superoinferior axis more prominently than the anteroposterior axis. LA demonstrates phasic volume changes during cardiac cycle representing reservoir, conduit (passive emptying), and contractile (active emptying) functions. Abnormal LA function is typically characterized by decreased compliance and/or contractile dysfunction.[5] Thickening of the wall and fibrosis may contribute to LA dysfunction by increasing the stiffness of the LA with or without significant dilatation.[6]

LAA enlargement often accompanies LA dilatation. Diminished LAA contractile function is characterized by diminished emptying velocity and stasis. The LAA has contractile and endocrinological functions, while its distensibility contributes to LA pressure modulation.[3,7]

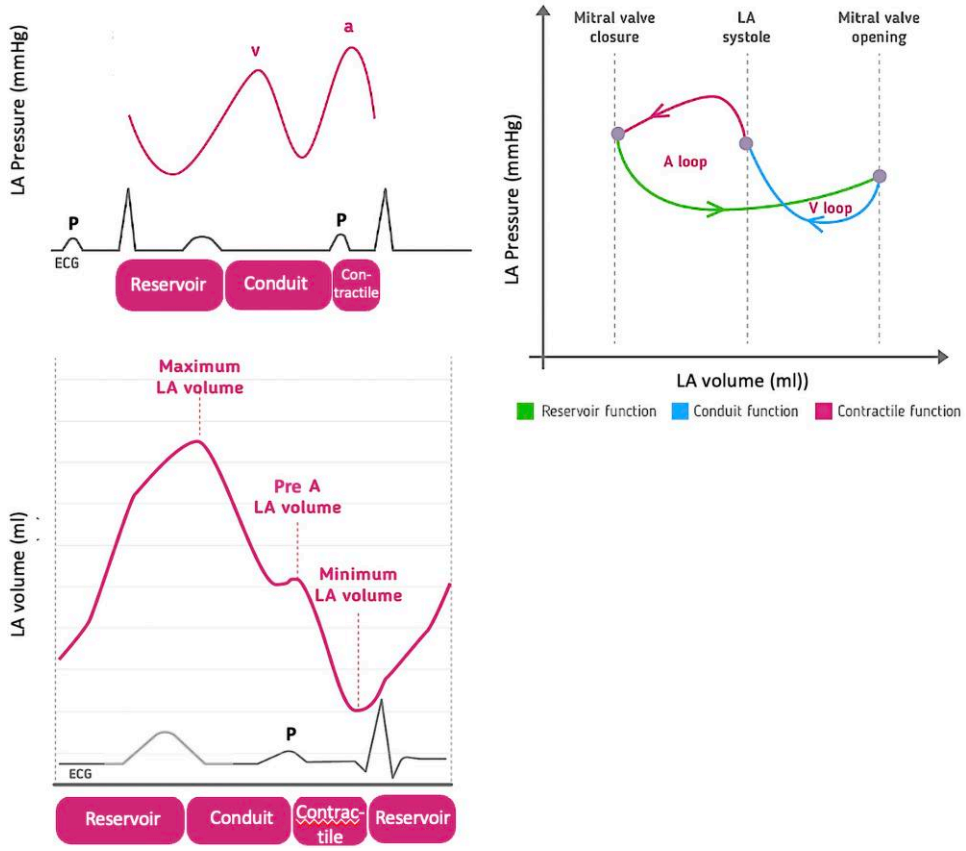

Figure 1 Phasic changes of LA: pressure, volume, and pressure/volume curves.

Multi-modality imaging for LA and LAA

The assessment of structural, architectural (tissue characteristics), functional, or electrophysiological changes associated with LA cardiopathy relies on the rational use of imaging modalities by appreciating their capabilities and limitations to derive clinically relevant information (*Table 1*).

Transthoracic echocardiography

Transthoracic echocardiography (TTE) is the primary imaging modality to evaluate LA size and function. Since LA enlargement is asymmetrical, anteroposterior LA diameter measured from the M-mode or 2D parasternal long-axis image can significantly underestimate LA size.[8,9] Yet, for some specific clinical conditions, the cut-offs for LA dilatation remain based upon anteroposterior linear measurements, such as in risk stratification in hypertrophic cardiomyopathy (HCM).[10,11] LA volume quantification by 2D echocardiography (2DE) and, preferentially, by 3D echocardiography (3DE) is the accurate way to evaluate LA size in clinical practice.[12] The measurement of LA volume by 2DE requires the acquisition of LA-focused apical views to maximize both the LA width and length in four- and two-chamber (should be similar in both views) to avoid foreshortening,[10] because the LA and the LV are not co-axial.[13] The bi-plane area–length method systematically yields larger LA volumes than the Simpson's bi-plane disc summation method as it assumes an ellipsoid shape.[14] The Simpson's method is preferred over the area–length method for clinical use because of fewer geometric assumptions than the area–length method.[5] LA volume calculated by 2DE correlates well with measurements obtained using 3DE, cardiac computed tomography (CCT), and cardiac magnetic resonance (CMR), despite some degree of systematic underestimation.[15] Automated tools based on 2D speckle-tracking echocardiography (STE) have high feasibility and yield LA volumes (average bias 1.5 mL, limits of agreement ± 8 mL) comparable to the standard manual tracing of LA endocardial contours.[15] By 2D echo, the upper limit of normal LA volume is defined as 34 mL/m^2 (range 16–34 mL/m^2) in both men and women.[10] Transthoracic 3DE has lower interobserver variability and higher accuracy than 2D, by avoiding foreshortening, geometric assumptions, and manual contour tracing errors.[16,17] LA volumes are significantly larger when measured by 3DE than by 2DE; therefore, cut-offs for detecting LA remodelling and dysfunction cannot be used interchangeably between the two techniques. Reference values for 3DE have been obtained from large cohorts of healthy volunteers (*Table 2*).[13,18,19] Recent studies testing the latest 3DE software tools dedicated for LA quantification showed that the measurement bias against CMR data is minimal and clinically negligible.[15,20] Fully automated 3D LA volume quantification using dedicated software packages also enables single-beat acquisitions with sufficient temporal resolution for reliable quantification of the LA even in patients with irregular rhythms.[21]

Maximal LA volume has been the most clinically used parameter; yet, there is an important body of evidence supporting the role of phasic LA volumes (particularly LA minimal volume) and function. LA function may demonstrate alterations prior to volume changes.[12] The same dedicated 2DE views used for maximal LA volume calculation can be employed to obtain LA phasic function parameters. From the LA volumes, the total emptying volume (EV) is calculated as (LAVmax – LAVmin), the passive EV as (LAVmax – LAVpreA), and the active EV as (LAVpreA – LAVmin). Total emptying fraction (LAEF); (total EV / LAVmax), passive LAEF;

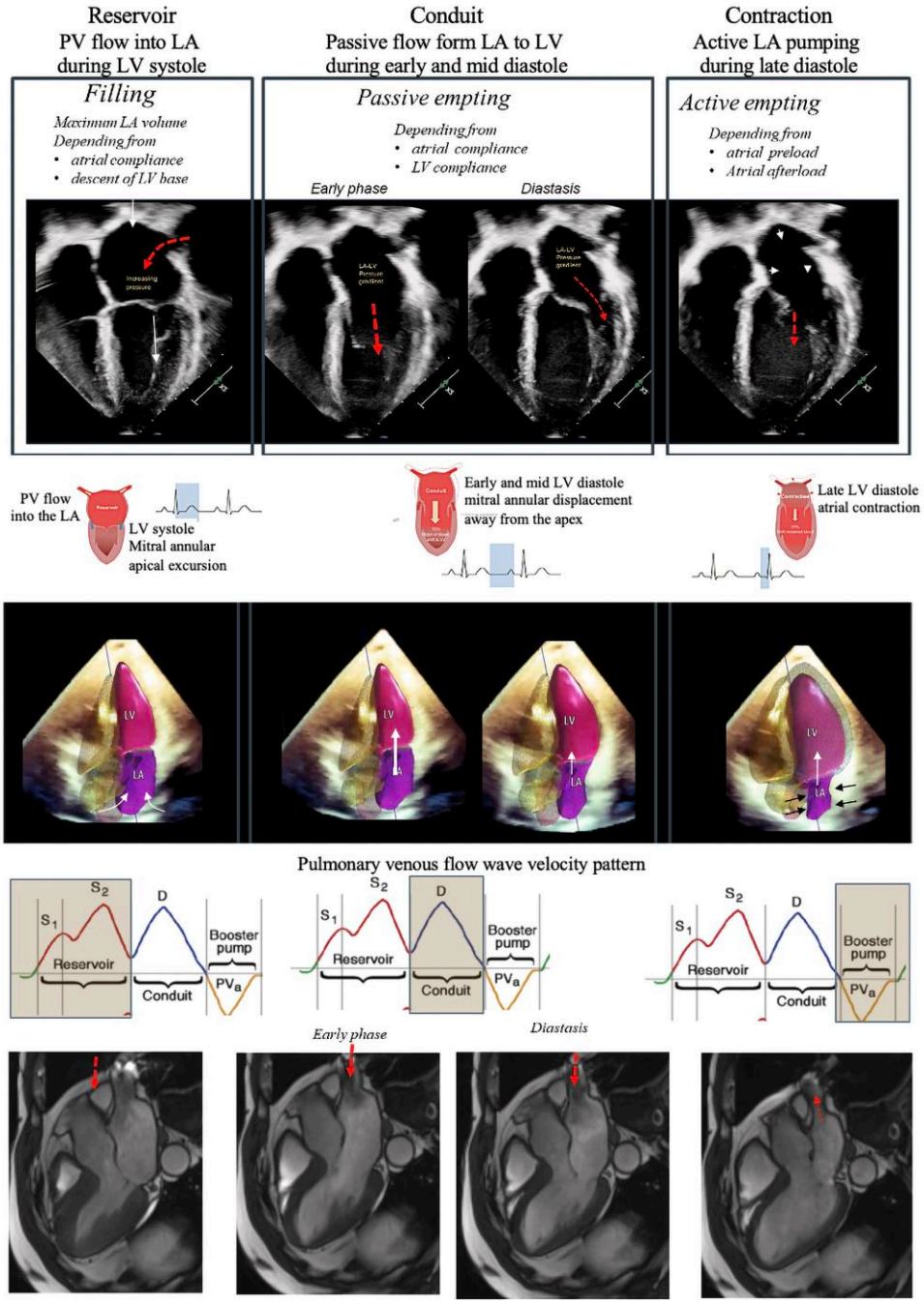

Figure 2 Translation of LA phasic function into imaging. Note the interaction between mitral annular descent by LV contraction, LA reservoir, atrial contraction, and PV flow.

(passive EV / LAVmax), and active LAEF; (active EV / LAVpreA) are calculated as indices of reservoir, conduit, and contractile function, respectively (*Figure 3*).[13] Because indexing LA size to body surface area accounts for gender difference, only the indexed value should be reported.[22]

Because of manual endocardial border tracing at three different time points of the cardiac cycle, assessment of LA phasic function by 2DE is time-consuming and prone to errors. LA function can be measured faster and automatedly, without geometric assumptions by using dedicated software packages for LA volume quantitation from 3DE datasets (*Figure 4*).[13] The limitations of 3DE at present include low spatial resolution and the need for dedicated equipment and training. There is paucity of data regarding its incremental prognostic value compared to 2DE.

Mitral inflow velocity during atrial contraction (A wave) and late diastolic mitral annular velocity (a′) are Doppler metrics of LA function. Blunted or absent A and a′ waves during sinus rhythm are typical findings of atrial stunning. Of note, these parameters are load- and angle-dependent and present during sinus rhythm only. Speckle-tracking strain has been a highly sought-after technique for LA function quantification. It is semi-automated, less angle-dependent, and less affected by artefacts than tissue Doppler-based measurements. LA strain

Table 1 Goal-directed multi-modality imaging for LA and LAA

	TTE	TOE	ICE	CCT	CMR	PET
LA volume	+++[a]	+	+	+++	+++	-
LA morphology	+++[a]	-	+	+++	+++	-
LA phasic function	+++[a]	-	-	++	+++	-
LA strain	+++	-	-	+	++	-
LAA morphology	-	++	++	+++	++	-
LAA function	-	+++	+	-	+	-
Pulmonary vein flow	++	+++	-	-	-	-
Pulmonary vein pattern	-	++	++	+++	+++	-
LAA thrombus	-	+++	+++	+++	++	-
LA fibrosis	-	-	-	-	++	++[b]
Peri-atrial epicardial fat	+[c]	-	-	+++	+++	-
Real-time image integration with EAM	-	-	-	+++	+++	-
Inflammation	-	-	-	-	-	++[d]

Abbreviations: CCT, cardiac computerized tomography; CMR, cardiac magnetic resonance; EAM, electroanatomic mapping; ICE, intracardiac echocardiography; PET, positron emission tomography; TTE, transthoracic echocardiography; TOE, transthoracic echocardiography.
[a]Ideally by 3DE.
[b]PET with fibroblast activating protein inhibitors.
[c]Only thickness.
[d]PET with fluorodeoxyglucose.

Table 2 Reference echocardiographic values of LA volumes[13]

	3D			2D
	Women	Men	Overall	Overall
LAVImax (mL/m^2)	31 (27–45)	31 (19–52)	32 (28–36)	24 (21–28)
LAVImin (mL/m^2)	10 (5–18)	11 (4–21)	10 (8–12)	8 (6–10)
LAVIpreA (mL/m^2)	18 (10–30)	18 (9–32)	18 (14–21)	14 (12–18)
Total LAEF (%)	68 (53–79)	66 (51–80)	67 (63–71)	67 (62–74)
Active LAEF (%)	40 (18–61)	41 (20–60)	41 (35–48)	46 (39–53)
Passive LAEF (%)	45 (22–60)	43 (23–61)	44 (38–49)	41 (32–48)

Values are given as median (Interquartile range). Abbreviations: LAVI, left atrial volume index; max, maximum; min, minimum.

assessment requires dedicated, focused image acquisitions to optimize lateral and temporal resolution. The use of dedicated software with an automated LA wall detection algorithm improves measurement reproducibility. The region of interest (ROI) should fit in the thin wall, accurately track the motion of the mitral annulus, and avoid the strong signals of the adjacent and stationary pericardial tissue, which—if included—may underestimate strain values.[23] LA function parameters [reservoir (LASr), conduit, and contraction strain] are computed as LA time–strain curves over the cardiac cycle (*Figure 5*). Analysis, reporting, and interpretation should follow the EACVI/ASE/Industry Taskforce consensus statement on LA strain analysis.[24] The reference timing of zero strain should be set at end-diastole (R–R gating). The alternative method is when zero strain is set at the onset of atrial contraction (P–P gating). Importantly, however, the R–R gating is less prone to errors

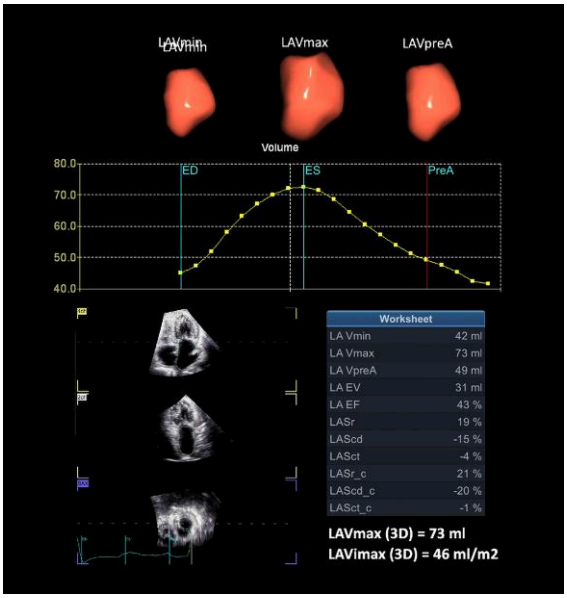

Figure 3 Phasic volumes by 3DE.

than the P–P gating and can be used during AF. Yet, high reproducibility (intraclass correlation 0.93 and 0.90, respectively) of both methods was shown in the MASCOT-HIT study.[25] Strain rate during ventricular systole, early diastole, and late diastole correspond to reservoir, conduit, and contractile function, irrespective of the R–R or P–P gating. Of note, LA load impacts volume and strain measurements regardless of the method used. Normal LA phasic strain values were reported in the healthy population from a meta-analysis including 40 studies in 2017 and from the NORRE study in 2018[19,26] (*Table 3*).

Additionally, reference ranges of LA phasic function by strain were published from 1329 healthy participants in the HUNT study (analyses performed by General Electric HealthCare EchoPAC system). Accordingly, bi-plane mean ±2SD reference values are as follows, in females and males, respectively: %LASr, 33.2 (17.2–49.2), 32.7 (16.0–49.3); %LA conduit strain, −17.0 (−30.8 to −3.3), −15.7 (−29.1 to −2.3); %LA contraction strain, −16.2 (−25.4 to −7.0), −17.0 (−26.9 to −7.0).[27]

Combining early diastolic mitral inflow (*E*) and annulus (*e′*) velocities with LASr enables obtaining an index for the estimation of LA stiffness by the formula: *E*/*e′*/LASr.[28]

Advice table 2 Use of TTE

Evaluation of the LA by TTE requires the acquisition of atrial-focused views.	
It is advised to assess LA size by volume (bi-plane 2D or 3D) quantification and to use the same tool for intra- and inter-individual comparisons.	
LA phasic volumes and strain by TTE are the mainstay of assessing LA function.	
Volumetric cut-offs obtained from different echo techniques cannot be used interchangeably.	
R–R gating is advised for the assessment of LA phasic function by 2D strain.	
LA size estimation should not be limited to M-mode or 2D linear measurements.	

Transoesophageal echocardiography

Transoesophageal echocardiography (TOE) is well suited to image the LA and the LAA, given their proximity to the oesophagus. However, LA sizing is performed by TTE rather than TOE, because the ultrasound scan sector cannot entirely encompass LA on TOE. Exclusion of thrombi, search of cardioembolic sources, characterization of the PVs before AF ablation, procedural planning, and guidance for LAA occlusion are the most common indications for imaging LA and LAA by TOE.[29] Although TOE is semi-invasive, it is safe in renal insufficiency. It provides adequate image quality in AF and offers information about associated cardiac pathologies and haemodynamics.

Technical considerations

Multiple TOE planes are used to explore the LA and LAA from the mid-oesophageal view. With 2D probes, LAA can be easily visualized between 45 and 90° with counterclockwise rotation and gentle anteflexion of the transducer. Once the LAA is visualized, it is centralized on the screen, and a thorough evaluation is performed by sweeping from 0 to 135°. However, 3D probes allow visualization of bi- or tri-plane simultaneously which facilitates the sweep process (*Figure 6*). A 3D zoom acquisition with a wide sector (since high temporal resolution is not specifically required for atrial structures) and excluding the atrial roof in the nearfield (avoiding obstruction of the view) is generally performed for a live assessment and further cropping. From the 3D zoom acquisition, a live 'en face' view of the LAA orifice can be obtained. Further perpendicular cropping and orientation of the 3D dataset enable the characterization of the LAA morphology. Photo-realistic rendering with light adjustments or CCT-like rendering with improved transparency (Glass) has also been recently introduced to improve the qualitative assessment by highlighting the tissue–blood interface (*Figure 7*).[30]

The TOE also provides anatomic and functional information about PVs. Notably, TOE underestimates PV dimensions, especially for the inferior veins.[31] The left upper PV is visualized in its long axis adjacent to LAA with further counterclockwise rotation between 45 and 110°. Visualization of the left lower PV requires slight vertical manipulation or further angulation to 120°. The right upper PV can be visualized after clockwise rotation of the probe with anteflexion from either 0, 45, or 120–135° (on the left and right side of the screen, respectively) adjacent to the IAS and superior vena cava. The right lower PV is the most difficult to align with the Doppler beam and is best seen from the extreme clockwise rotation of the probe at 0° without anteflexion immediately inferior to the right upper PV. PV Doppler interrogation shows systolic (S), diastolic (D), and atrial contraction (A) waves during sinus rhythm (*Figure 8A–D*). PV flow velocities are relevant for the assessment of LA pressure, mitral regurgitation (MR) severity, and PV stenosis after PV isolation. The left and right PV orifices are widely separated, and the pyramidal 3D data set cannot include them all in a single image. From the best 2D views obtained, the left and right PV orifices can be seen 2 by 2 by 3D zoom acquisition from an optimal orthogonal display, and rotation of the dataset as shown in figure (*Figure 8E* and *F*). The left PVs are adjacent to LAA, and the right PVs run adjacent to the IAS.

LAA function

Flow in the LAA is visualized using colour Doppler with a low Nyquist limit, and flow velocities are measured by pulsed-wave Doppler. Four phases have been described: emptying (contraction) velocity, filling velocity, a biphasic systolic reflection wave, and an early diastolic emptying wave[29] (*Figure 9*). Emptying velocity ranges from 63 ± 29 to 83 ± 25 cm/s and filling velocities range from 54 ± 17 to 61 ± 18 cm/s. Velocities can decrease because of high LA pressure. A sawtooth pattern with low velocities is observed during AF. Velocities <40 cm/s in sinus rhythm are associated with an increased risk of stroke.[32]

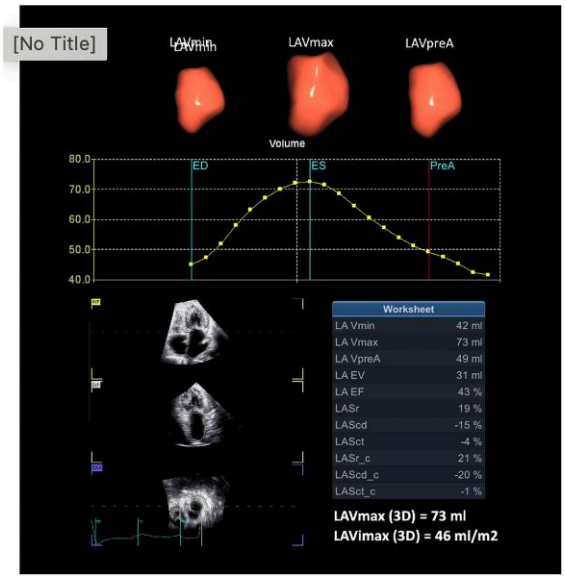

Figure 4 3D automated LA volume quantification. Note that the LA long axis is adjusted.

Advice table 3 For the use of TOE

Multiplanar imaging with or without 3D is indispensable for complete visualization of LAA morphology.	
TOE is the preferred technique for the assessment of LAA, function, and thrombus.	
TOE is the preferred technique for the assessment of PV flow.	
The use of TOE is inappropriate for the assessment of LA size or volume.	

CMR

CMR allows a comprehensive 3D evaluation of LA anatomy, structure, and function. Its potential to reveal the extent of atrial fibrosis by late gadolinium hyperenhancement (LGE) imaging is an advantage.[33]

Assessment of morphology

CMR steady-state free-precession (SSFP) cine images provide excellent blood-endocardium and epicardium-fat contrast, allowing good delineation of the atrial endocardial borders and LA size. This allows precise measurement of LA volumes, either using a bi-plane area–length method from two- and four-chamber cine images (*Figure 10A*) or using the Simpson's disc summation method on a stack of adjacent short-axis images from the atrioventricular ring to the roof of the LA. Since LV and LA are not co-axial, the LA volumes derived from the bi-plane area–length method may underestimate the true LA size because the long-axis cine images are normally aligned to the LV axis during

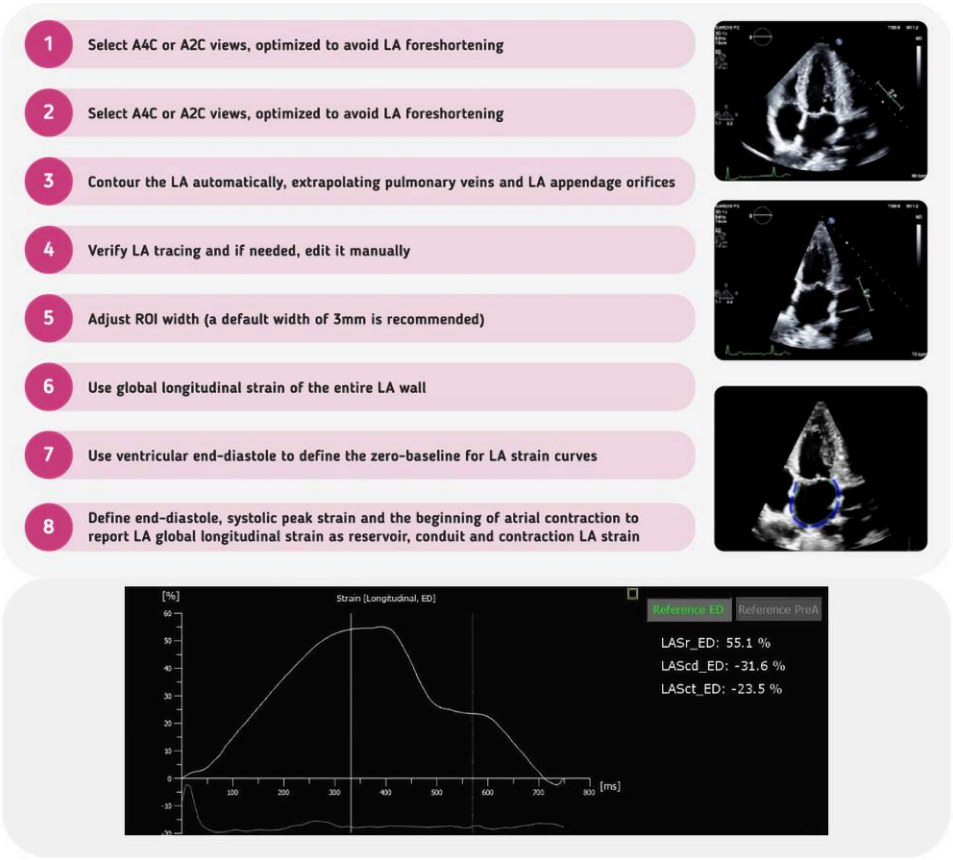

Figure 5 Image acquisition and computation of LA strain.

Table 3 Reference values of LA phasic strain (NORRE study)[19]

	All ages	Age 20–40 years	Age 40–60 years	Age >60 years
LAS reservoir	42.5 (36.1–48.0)	46.8 (42.3–52.4)	40.9 (35.4–46.1)	35.5 (30.9–41.9)
LAS contraction	−16.3 (−12.9 to −19.5)	−15.6 (−11.9 to −19.0)	−16.3 (−13.2 to −19.6)	−16.8 (−13.6 to −21.4)
LAS conduit	−25.7 (−20.4 to −31.8)	−30.6 (−26.8 to −36.5)	−24.1 (−19.7 to −29.3)	−18.6 (−14.7 to −22.6)

Values are given as median (interquartile range).

acquisition. The Simpson's method is more precise and overcomes the geometric assumption and limitations of the area–length method; however, it requires additional scanning time to acquire the LA short-axis stack. The reference values obtained from the two- and four-chamber cine images are given in *Table 4*.[34]

More precise evaluation of atrial morphology, especially of the LAA and PV, can be achieved by using 3D angiographic (MRA) images (*Figure 10C*) which can be acquired either using free breathing of navigator gated MRA after gadolinium injection or using non-contrast balanced SSFP MRA.[35] Like CCT, these images can be merged with 3D electro-anatomical maps using landmarks or surface registration for AF ablation[36] (*Figure 10E*). Evaluation of the anatomy of the PV pre-ablation and PV stenosis post-ablation is also feasible with CMR; however, less data is available as compared to CCT.[37]

CMR allows understanding of tissue characteristics and detection of atrial fibrosis by high-resolution 3D LGE imaging[38] (*Figure 10E*). LGE on the LA wall has been detected in several conditions such as AF,[39,40] mitral valve diseases,[41] and cardiac amyloidosis (CA).[42] Yet, assessment of atrial LGE is performed visually at best by experienced centres without a consensus for quantification and is not possible if the image quality is suboptimal. Variability among observers has been a significant disadvantage.[38] Further work is required to standardize atrial LGE imaging to enable its widespread clinical use.

Cine and 3D MRA allow also the assessment of LAA size and morphology and measurement of its ostial diameter and depth. For assessing LAA thrombus, CMR with inversion time myocardial delayed enhancement acquisition has the highest accuracy (99.4%) followed by contrast-enhanced (97.6%) and cine CMR 93.9%) tools.[43] Hence,

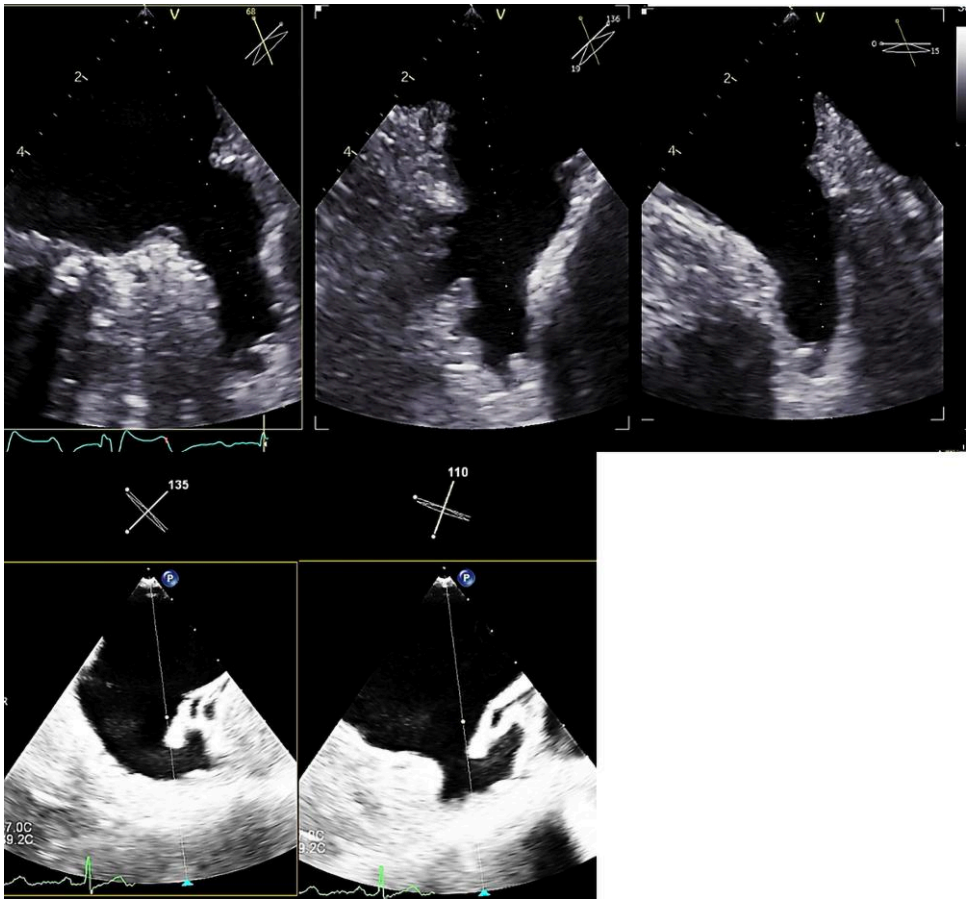

Figure 6 Multiplane images of the LAA showing different morphologies.

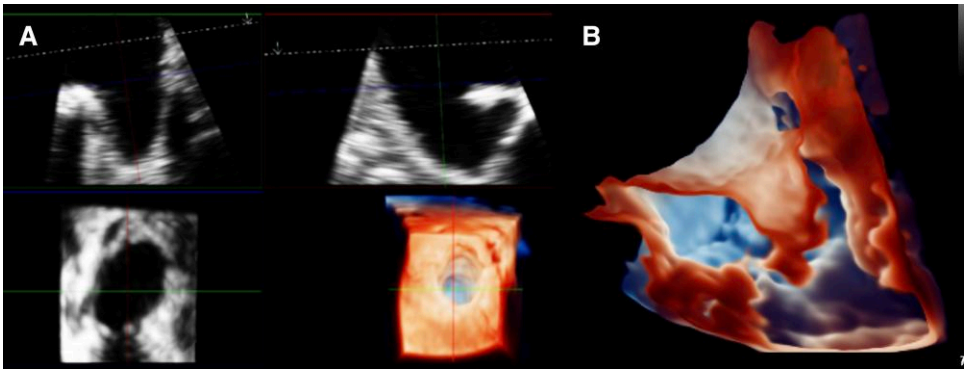

Figure 7 (*A*) Zoom-mode acquisition and multiplane display of LAA morphology by cropping and re-orienting the 3D data set with 3D photo-realistic rendering. (*B*) Glass view of the LAA.

CMR is an alternative to TOE or CCT in centres having adequate experience in LAA image acquisition and interpretation, depending on the resources.

Finally, CMR (T1-weighted or cine SSFP images) can accurately quantify the volume and area of pericardial adipose tissue.[44] A recent meta-analysis showed that LA epicardial adipose tissue (EAT) thickness was a strong parameter associated with the risk of AF recurrences after catheter ablation.[45]

CMR may suffer from artefacts in case of AF with high heart rate and devices (particularly intracardiac defibrillator).

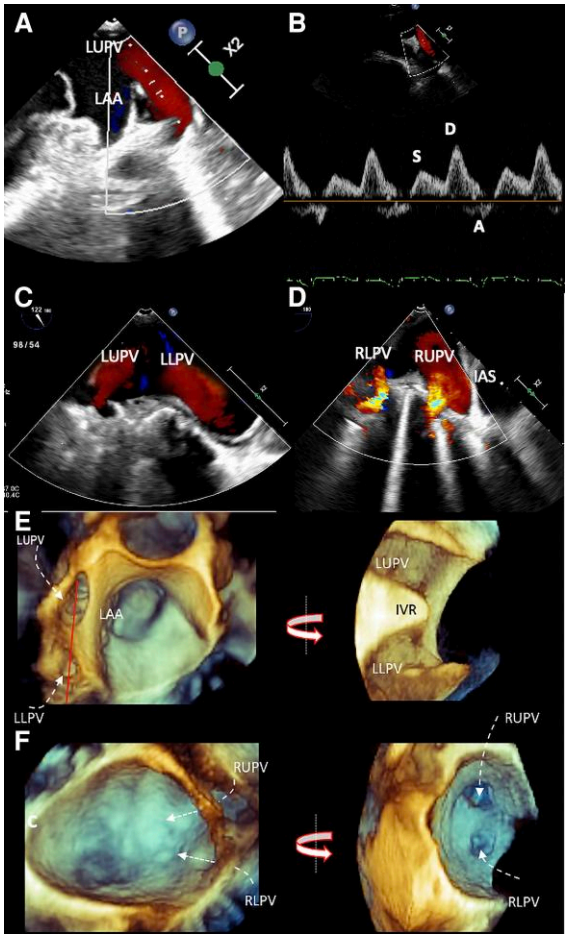

Figure 8 PVs by TOE. (*A*) Left upper PV, 60°, colour Doppler; (*B*) left upper PV, pulsed-wave Doppler; (*C*) left upper and lower PVs, 120°, colour Doppler; (*D*) right upper and lower PVs, 0° clockwise rotation; (*E*, *F*) the left and right PVs, 3D-rendered image.

Assessment of function

LA function can be assessed with CMR by computing LAEF from measurements of maximum and minimum volumes and phasic LA volume–time curves from the cine images (*Figure 10B*) (*Table 4*).[34,46,47] Recent technology enabled LA strain quantification by automated feature tracking methods from two- and four-chamber cine images (*Figure 10D*). A recent meta-analysis showed that feature tracking vendor matters for the heterogeneity of measurements rather than the CMR vendor, sex, and age.[48] The pooled mean values of LA phasic strain are presented in *Table 5*. There are promising advances in measuring peak velocity and vorticity by 4D flow imaging paving the way for the assessment of atrial haemodynamics[46,49] (*Figure 10F*).

CCT

Due to its excellent spatial resolution, CCT plays a pivotal role in defining the morphology of the LA, LAA, PVs, and function of the LA and in guiding electro-anatomical mapping. For evaluating LA, PVs, LAA morphology, and epicardial fat, a single arterial phase acquisition with ≥64-slice CCT with ECG triggering is required. Prospective ECG triggering is used in patients with sinus rhythm and low heart rate whereas retrospective ECG triggering is appropriate in patients with high and non-stable heart rates.[50] In patients who are in AF during the scan, acquisition is more challenging, but the introduction of more recent technology allows adequate image quality even during AF.[51,52] *Figure 11* shows a typical 3D LA reconstruction with CCT. An additional delayed scan after contrast injection is mandatory for ruling out LAA thrombus.[53] While the time to delayed images varied in studies, most were acquired 30–180 s after the initial images.

Assessment of morphology

CCT has a higher spatial resolution than CMR and is a well-established technique to evaluate LA and LAA morphology and volume and PV patterns, to rule out LAA thrombus, and to detect peri-atrial adipose tissue.

CCT systematically detects higher LA volumes compared to 2DE and CMR because of several reasons.[54] First, due to higher temporal resolution, the proper image reconstruction windows for

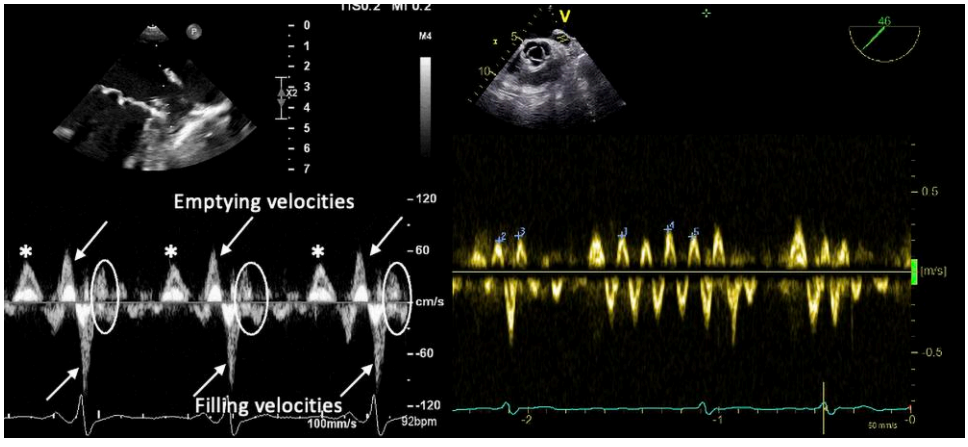

Figure 9 Normal quadriphasic wave pattern of LAA flow. Early diastolic emptying (asterisk), systolic reflection (circles) waves.

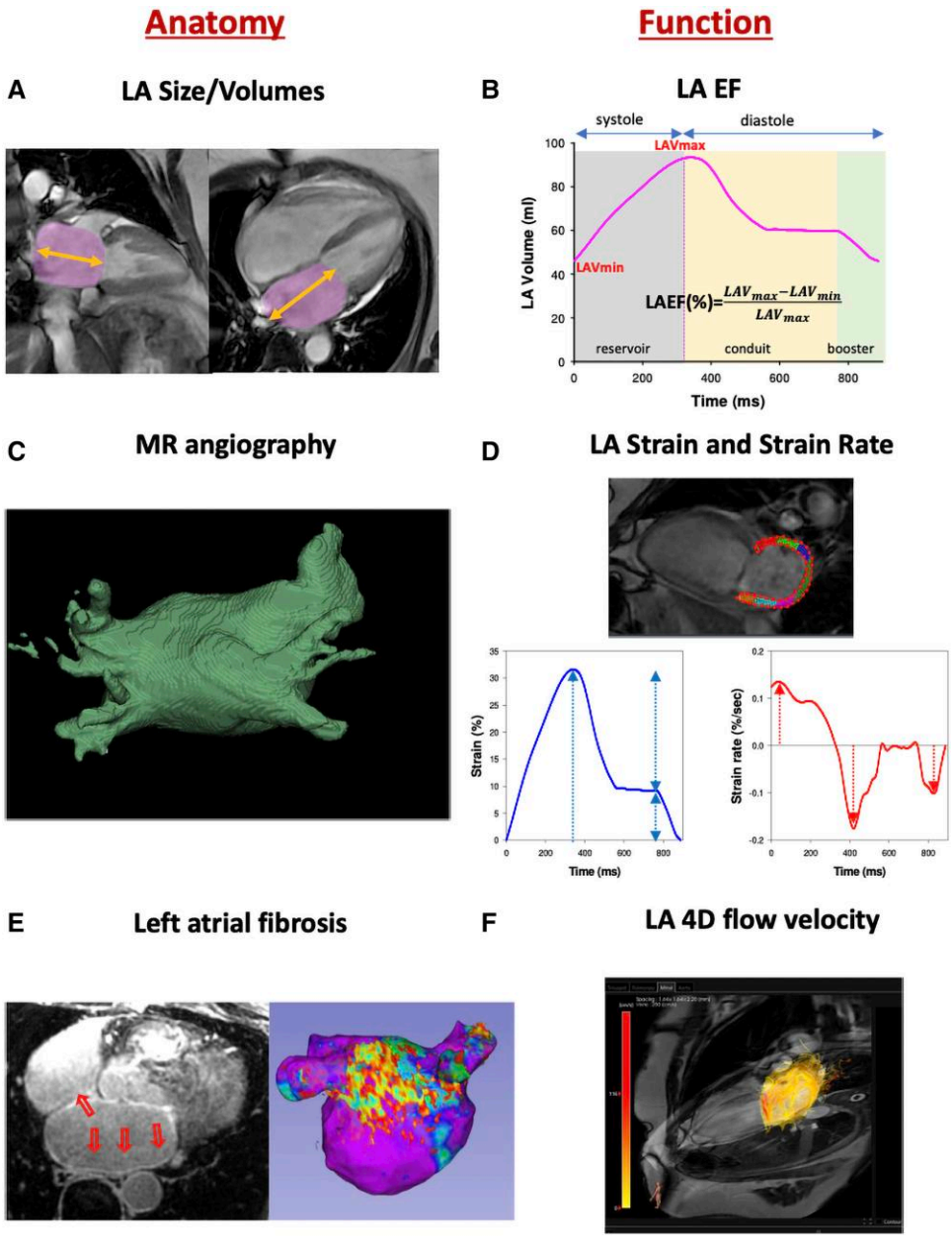

Figure 10 LA by CMR. (*A*) Area–length method from two- and four-chamber cine images. (*B*) Computation of reservoir, conduit, and contractile function and emptying fraction. (*C*) 3D anatomy by contrast or non-contrast-enhanced magnetic resonance angiography (MRA). (*D*) LA strain and strain rate. (*E*) LA fibrosis (arrows) by LGE and the computation of 3D maps of atrial fibrosis. (*F*) The myocardial blood flow distribution and velocity by 4D phase contrast.

accurate measurement of LA volume could be more achievable with 2D echo or CMR rather than CCT. Second, image noise during systolic phase may contribute to the overestimation of LA volume by CCT. Third, bolus injection of high-volume iodine contrast agent at high-rate infusion or drugs usually used for CCT scan such as β-blockers could modify LA morphology transiently, partly by incorporating more PV volume. *Table 6* represents the normal reference values of LA volumes by gender from 569 healthy subjects undergoing 320-detector CCT as a part of the Copenhagen General Population Study.[55]

CCT is now recognized as a good alternative for detecting LAA thrombus. Romero *et al.*[53] described a diagnostic accuracy of 94% of CCT vs. TOE to rule out LAA thrombus with 41% positive predictive value, because incomplete opacification of the LAA is common in patients with AF mimicking thrombus in acute phase scans. The positive predictive value increased to 92% with an overall diagnostic accuracy of 99% if delayed contrast imaging (venous phase) is added to arterial phase acquisition (*Figure 12*). CCT also clearly differentiates LAA morphologies as cactus, chicken wing, windsock, or cauliflower pattern.[56]

Contrast-enhanced CCT has potential for tissue characterization. Distribution of hypoattenuation is one way by which CT can identify myocardial fibrosis.[57] Also, new methods to perform extracellular volume quantification using CT are emerging.[58] CCT is the preferred

Table 4 Reference values of LA by CMR[34]

	Men		Women	
	Mean ± SD	Lower–upper limits	Mean ± SD	Lower–upper limits
Bi-plane LAVImax (mL/m^2)	38 ± 11	17–59	39 ± 11	17–61
Bi-plane LAVImin (mL/m^2)	14 ± 5	3–24	13 ± 5	4–23
Bi-plane LA EF (%)	62 ± 8	46–77	63 ± 8	48–78
Simpson LAVImax (mL/m^2)	41 ± 8	24–57	44 ± 8	28–60
Simpson LAVImin (mL/m^2)	19 ± 5	9–28	19 ± 4	11–27
Simpson LA EF (%)	54 ± 8	38–70	57 ± 6	45–69

Abbreviation: SD, standard deviation.

Table 5 LA strain reference values by CMR feature tracking[48]

	Mean	95% CI
LAS reservoir %	34.9	29.6–40.2
LAS conduit %	−21.3	−16.6 to −26.1
LAS contraction %	−14.3	−11.8 to −16.8

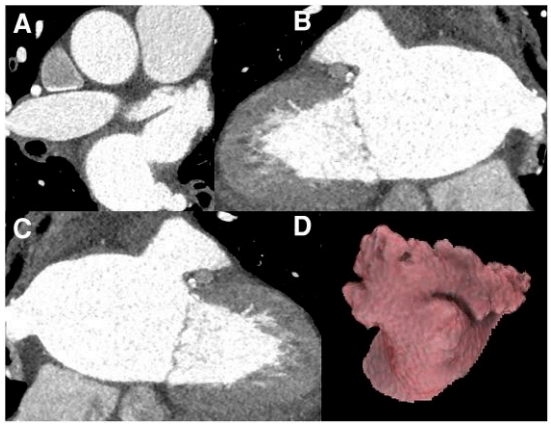

Figure 11 LAA. (*A*) Axial, *B*) sagittal oblique, *C*) coronal oblique views, and *D*) 3D volume-rendered image.

method to assess the PVs, although no differences are described between CCT and CMR in terms of diagnostic accuracy of PV pattern[51,54] (*Figure 13*).

CCT is accurate and reproducible to assess epicardial fat tissue (EFT) by either manual or semi-automated volume quantification. This latter algorithm defines all structures with contrast attenuation ranging between −195 and −45 HU as adipose tissue.[59] A volumetric quantification is advised rather than area measurements.[59] CCT also allows visualization of the peri-atrial anatomy for safe guidance of procedures and helps to avoid phrenic nerve injury or atrio-oesophageal fistula.[60,61]

Assessment of function

With ECG-triggered acquisition, functional series can be obtained in order to perform LA strain quantification. However, currently, data regarding LA strain assessment using functional CCT images are scarce. LA strain is usually obtained by tracing endocardial LA borders on multiple apical two-chamber views excluding LAA and PVs. Szilveszter *et al.*[62] demonstrated excellent intra-observer reproducibility for this approach with an intraclass correlation of 0.95, a correlation coefficient of 0.87, and 5.6 points of underestimation as compared to 2D echo. Yet, relatively low temporal resolution and radiation exposure limit the use of CCT for LA strain quantification in clinical practice.

Advice table 4 Use of CMR and CT

CMR is the gold standard for the quantification of peri-atrial adipose tissue volume.	
CCT is advised for assessing the anatomy of PVs.	
CMR and CCT are alternatives to echocardiography for the assessment of LA, LAA morphology, volume, and thrombus.	
Using the same imaging modality is strongly advised for intra- and inter-subject comparisons.	
CMR can be used as an alternative to CCT for assessing the anatomy of PVs.	
CMR with automated feature tracking can be used for LA strain quantification.	
CMR with LGE can be used for visualization of LA wall fibrosis with good-quality imaging, by the experts.	

Nuclear imaging

Molecular positron emission tomography (PET) imaging as a tool to assess atrial inflammation and fibrosis is in early stages. Increased atrial 18F-FDG uptake has been shown in patients with AF and in those with sarcoidosis as a predictor of subsequent AF.[63,64] More recently, 68Ga-fibroblast activation protein inhibitor (FAPI-PET) was used to detect increased fibroblast activation in the atria of patients with AF or after PV isolation.[65,66] Atrial activity is rarely reported but seems to be clinically relevant. Oncologic patients frequently have atrial uptake on their PET/CT which is also linked to the risk of AF and prothrombotic state with cardio-oncologic consequences.[64] Further investigations are awaited to consolidate clinical implications.

Table 6 Reference values (mean and 2.5–97.5%) for LAVI by CCT[55]

Age group	Men				Women			
	40–50	50–60	60–70	>70	40–50	50–60	60–70	>70
LAVImax (mL/m^2)	76 (47–108)	81 (53–118)	83 (44–114)	92 (67–154)	63 (43–91)	67 (49–96)	71 (49–102)	78 (55–124)
LAVImin (mL/m^2)	38 (25–54)	41 (27–58)	43 (21–63)	49 (36–74)	36 (25–50)	39 (28–54)	42 (30–56)	48 (38–77)

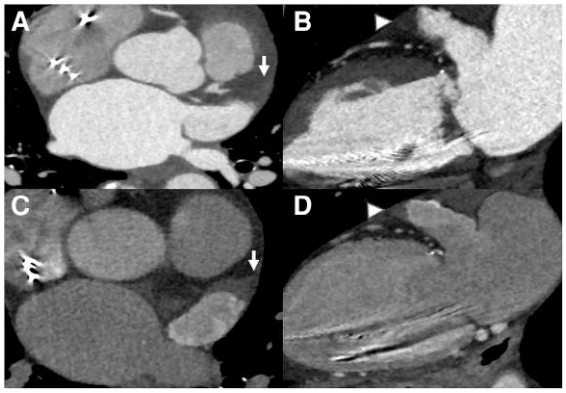

Figure 12 LAA thrombus. Arterial phase CCT scans (*A*, axial; *B*, oblique parasagittal three-chamber views) with endocavitary filling defect at the apex of the LAA, persisting into the late phase of imaging, 15 s later (*C–D*), consistent with thrombus (arrows).

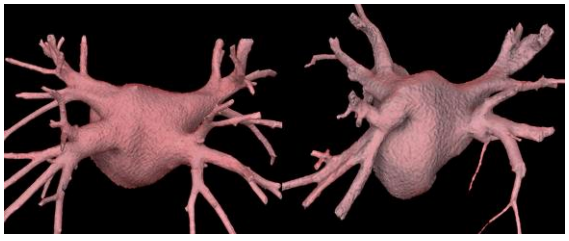

Figure 13 3D volume-rendered CT images of the LA. (*left*) Normal anatomy: four PVs draining into the superior posterior surface of LA. (*right*) A common anatomical variant characterized by the two left PVs draining into a common trunk.

Integration of LA imaging into diagnostic and prognostic evaluation

HF

Asymptomatic HF

The development of overt HF is preceded by HF risk factors with or without abnormal cardiac structure and function.[67] While LV structural (e.g. LV hypertrophy) or functional parameters [reduced EF or global longitudinal strain (GLS)] are classically used to define HF regardless of symptoms, evidence of atriopathy also seems to be a marker of HF. Thus, LA size (maximum and minimum volume) and function (LAEF, LASr, and LASct) might likely be incorporated into the definition of HF as an objective evidence of functional and structural abnormality. For example, in 1802 participants in the Dallas Heart Study, increasing left atrial volume index (LAVI) and decreasing LAEF were associated with hypertension and elevated brain natriuretic peptide (BNP), LAVI was most strongly associated with LVEDVi, and LAEF was associated with left ventricular ejection fraction (LVEF) and morphology. Reduced LAEF was independently associated with 8-year mortality in the general population and provided incremental prognostic utility to clinical risk factors, LV mass, and LVEF.[68] The availability of LA strain has made the detection of cardiopathy more feasible. In an analysis of 112 subjects with incident HF and 112 case–controls from the Multi-Ethnic Study of Atherosclerosis (MESA), atrial changes were present in CMR images obtained 8 years previously despite asymptomatic status. Specifically, subjects who developed HF had larger baseline LA volume index (40 ± 13 vs. 33 ± 10 mm^3/m^2, $P < 0.001$) and lower peak longitudinal LA strain (25 ± 11 vs. $38 \pm 16\%$, $P < 0.001$) years before. In fact, LASr was associated with incident HF independent of clinical risk factors, LV mass, and natriuretic peptides.[69]

HF with preserved ejection fraction and DD

During ventricular diastole, LA is exposed to the pressure of LV. With LV DD, LA pressure rises to maintain adequate LV filling, which in turn leads to dilatation and stretching of the LA wall. LAVI >34 mL/m^2 is one of the criteria for the diagnosis of DD.[70] However, LAVI has limitations during the early phases of DD.[71] In addition, LAVI increases with age and is modified by the percentage of age-predicted O_2 consumption (cardiorespiratory fitness).[72] Assessment of LASr in addition to the European Association of Cardiovascular Imaging (EACVI)/American Society of Echocardiography (ASE) criteria has been proposed for improving the diagnostic precision of the DD algorithm by decreasing the indeterminate cases.[73] LASr, unlike traditional parameters, deteriorates progressively with the severity of DD. Thresholds of LASr were proposed to separate normal from Grade 1 to 3 (35%), Grade 1 from 2 to 3 (24%), and Grade 3 from 1 to 2 DD (19%), respectively.[74]

While LAVI takes place in the algorithm of estimating LV filling pressure, LASr does not.[70,75] However, replacing a missing parameter in this algorithm with LASr (cut-off <18%) has been shown to facilitate the detection of increased filling pressure.[75] LASr is more sensitive in detecting elevated filling pressures even when LAVI is normal during sinus rhythm.[73,76] LASr <18% is associated with increased LV filling pressure (PCWP ≥15 mmHg) particularly if LVEF is <50%.[77]

Enlarged LAVI, reduced LASr, and GLS together with LV hypertrophy are supportive for the diagnosis of HF with preserved ejection fraction (HFpEF).[67,75] In the absence of a specific aetiology, recognition of DD and estimation of LV filling pressure are crucial for the diagnosis of HFpEF. Of note, the PARAMOUNT trial showed that LA phasic function and LASr are decreased independently of LAVI and the history of AF in HFpEF.[78] In the substudy of TOPCAT, LASr was associated with HF hospitalization and related to both LV systolic and diastolic function.[79] Although LASr is not cited among the diagnostic criteria of HFpEF,

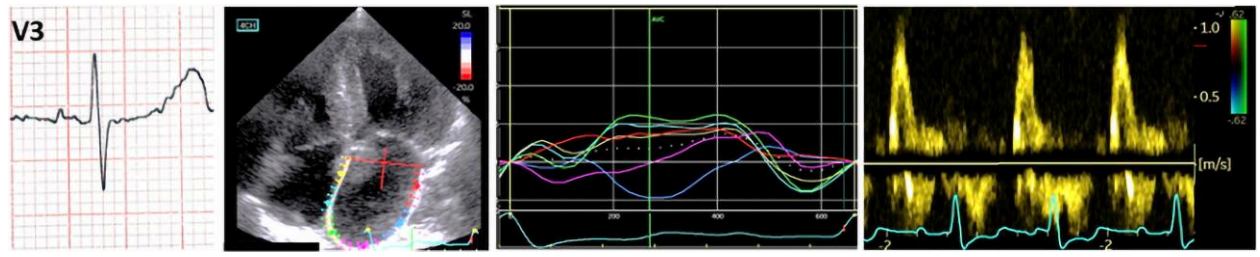

Figure 14 Atrial electromechanical dissociation in CA. Poor LA strain, absent LA contraction strain, and A wave, despite sinus rhythm.

abnormal LASr is associated with dyspnoea, NYHA class, and HF hospitalization and is a useful adjunct to the evaluation of DD and estimation of LV filling pressure algorithms in indeterminate cases.[73,79]

HF with mildly reduced and reduced EF

LA enlargement in HF with mildly reduced EF (HFmrEF) and HF with reduced EF (HFrEF) is associated with adverse cardiovascular events.[80] However, the impact of LASr on outcomes, in these patients, has been less studied. The best relationship between LASr and filling pressure is found in patients with reduced systolic function.[77,81] HFmrEF (EF = 41–49%) by definition needs the presence of symptoms and/or signs of HF. The presence of increased LAVI, elevated natriuretic peptides, and evidence of structural heart disease make the diagnosis more likely, but are not mandatory for diagnosis.[82]

Ischemic heart disease

Patients with ischaemic heart disease or after myocardial infarction (MI) make up the largest Stage B HF group. Accordingly, LA function and remodelling could be a marker of abnormal cardiac function with a diagnostic value. Additionally, LA function has been shown to predict HF hospitalizations after MI[83] and was incremental to LAVI.[84] A recent large CMR study showed that LAEF is independently associated with increased mortality in patients with ischaemic cardiopathy (LVEF <50%) even after adjusting for infarct size and MR severity.[85] LASr, assessed within 48 h of acute MI, was associated with the composite outcome of death and HF[86] and provided incremental value to LAVI in patients treated with percutaneous coronary interventions.[87] Data from multicentre prospective CMR studies [AIDA STEMI (NCT00712101) and TATORT NSTEMI (NCT01612312)] also showed that LASr (cut-off of 18.8%) is an independent predictor of outcome and incremental to LVEF, GLS, microvascular obstruction, and infarct size.[88] LAVI predicted morbidity and mortality after acute MI as well.[89,90] However, LA dilatation reflects a chronic process therefore may not be an ideal marker shortly after an acute MI in contrast to the indices of LA function that correlate more strongly to LV filling pressure after acute MI. Additionally, reduced LASr was shown to predict an increased risk of new-onset AF after coronary artery bypass graft surgery.[91]

Athlete's heart

LA dilatation is triggered by the increase in preload during athletic training as an adaptive mechanism.[92,93] Age, type of sport, and duration and intensity of training influence the degree of atrial remodelling. LAVI is associated with higher cardiorespiratory fitness and maximal oxygen consumption during exercise in both men and women.[94] A systematic review including 7189 elite athletes and 1375 controls described increased LAVI in athletes with an upper limit of normal 35.8 mL/m^2 compared to <34 mL/m^2 in the general population.[95] Spencer *et al.*[96] reported LAVI exceeding 48 mL/m^2 in 40% of male and 32% of female athletes. Importantly, there is a balanced adaptation with global remodelling in both atria and ventricles. Despite LA enlargement, *E*/*e*′ remains normal by means of increased LA and LV compliances and bradycardia and maintains LA pressure within normal range.[96] Conflicting evidence from relatively small cohorts exists about reversal of LA dilation with detraining.[93,97] In athletes, LASr is either preserved or mildly reduced (39%; 95% CI, 38–41%) compared to untrained controls,[92] and LA active emptying is lower in athletes (17%; 95% CI, 16–19%). Athletic atrial remodelling seems to be dependent on the intensity of training.[98,99] Adaptation of phasic volume changes during exercise enables distinction between physiological and pathological atrial remodelling.[100] Moderate exercise appears to protect against AF, whereas strenuous exercise increases the risk of AF which is postulated to be mediated by atrial dilatation, vagal tone, exercise-related adrenergic stimulation, and augmented LA pressure during exercise.[101,102] Increasing intensity and duration of athletic training leads to atrial enlargement and reduced atrial strain; only subtle further changes occur with AF. Therefore, prediction of AF in athletes by LA volume and strain is challenging as evidenced by conflicting results.[103–105]

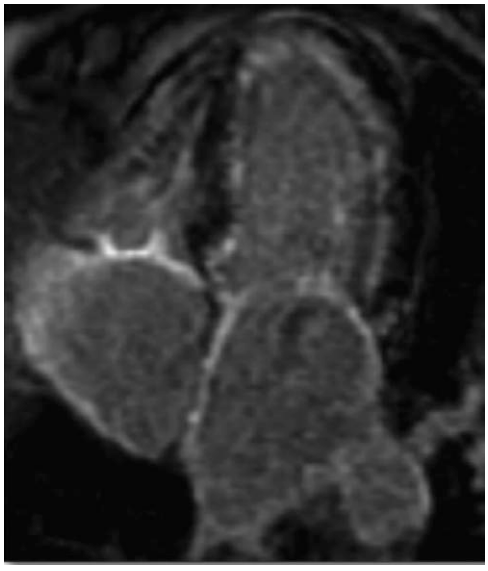

Figure 15 Diffuse LGE on the LA wall in CA.

HCM

LA remodelling is promoted by impaired LV filling and raised LA filling pressures in HCM. HCM may also cause direct LA cardiopathy as

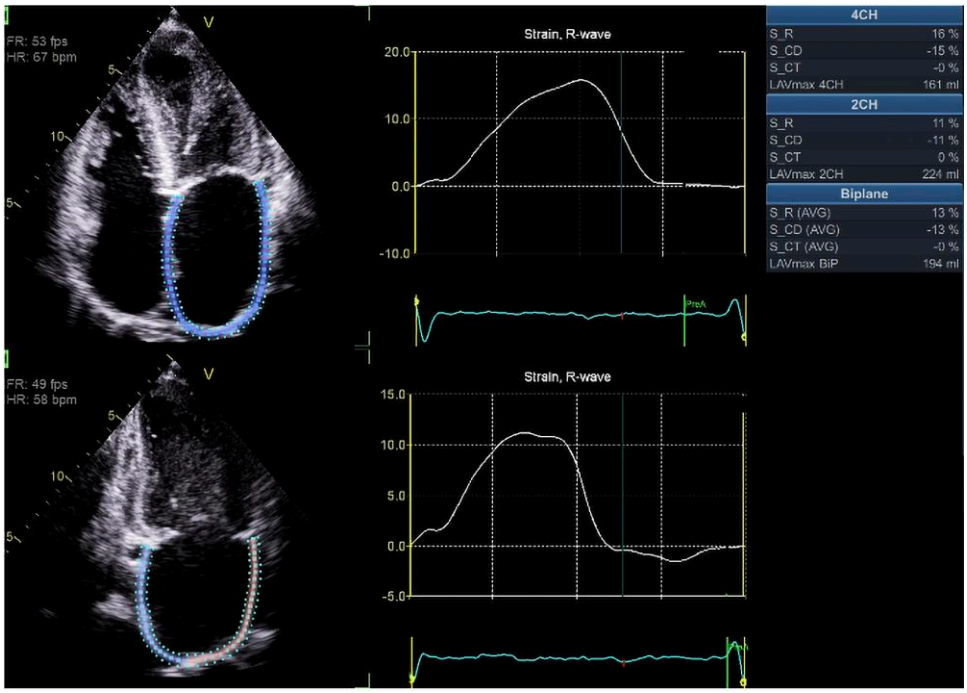

Figure 16 LA strain in AF. Note the lack of contraction; only the reservoir strain can be quantified which is significantly reduced.

evidenced by reduced passive and active LA emptying in the preclinical stage with positive genotype but without evident LV hypertrophy.[106] LA imaging and identification of AF risk are important because HCM is associated with a five-fold higher risk of AF incidence as compared with the general population and an increased rate of cardioembolism.[107] Increased LA volume, reduced atrial EF, and reduced LASr have been found to predict incident AF in the HCM populations.[108,109] A high burden of atrial LGE on CMR was reported in patients with HCM and AF.[110] Adverse LA remodelling in HCM has been shown to be a marker of poor outcome.[111,112] LA diameter is a component of the sudden cardiac death risk scoring system in HCM patients as validated in 2014.[113] The utility of more novel LA metrics has not been tested in identifying sudden cardiac death risk in large cohorts. Treatment of HCM is associated with LA structural and functional changes. Hegde *et al.*[114] documented reductions in LA volumes and improvement in LV diastolic function and natriuretic peptide levels after treatment with mavacamten. Finally, regarding the controversy of exercise training in HCM, a similar LAVI increase was observed with competitive exercise in athletes with and without HCM.[115]

CA

Both primary LA cardiopathy from amyloid accumulation-mediated damage and secondary involvement due to increased LV filling pressure, MR, and AF occur in CA.[116] Amyloid infiltration typically increases the thickness and stiffness of the atrial wall and IAS preventing excessive dilatation. Consequently, deformation-based parameters become more relevant than LA size for risk stratification in this population. Poor LASr and poor or absent LASct are typical findings in CA.[117] The increase in LA stiffness can be estimated by the ratio *E*/*e*′/LASr.[28] During ventricular systole, the LA acts as a non-distensible (stiff) reservoir causing increased LA pressures and reducing the energy stored in the walls which affects the conduit phase. Finally, a lack of atrial mechanical contraction can be observed in a proportion of the patients

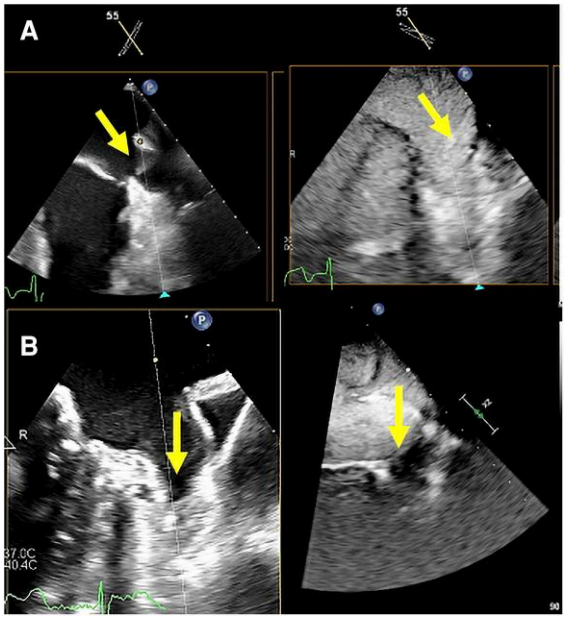

Figure 17 Ultrasound contrast for LAA opacification: (*A*) artefact mimicking thrombus, washing out with contrast, (*B*) thrombus producing a filling defect with contrast.

despite sinus rhythm, i.e. atrial electromechanical dissociation as a distinct feature and poor feature and poor prognosticator in CA (*Figure 14*).[116] LA strain is independently associated with high thrombotic risk in patients with CA.[118] LGE due to amyloid deposition or fibrosis in the LA wall can be detected by CMR[42] (*Figure 15*) and is

Table 7 Clinical characteristics of SEC, sludge, and thrombus[56]

	SEC	Sludge	Thrombus
Prevalence	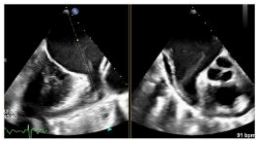 ≈50%	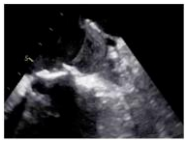 1–14%	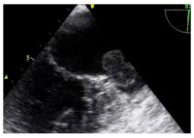 13%
Echocardiographic characteristics	Smoke-like echogenicity with variable density. Grade 1: minimal dynamic echogenicity in the LAA or sparely distributed in the LA; transient during cardiac cycle; Grade 2, swirling pattern with similar distribution to Grade 1; Grade 3, constantly detectable dense swirling pattern in the LAA that spills into the LA with less dense intensity; Grade 4, very slow swirling dense smoke-like echoes in the LAA, extending with similar density into the LA. Full, opacification with contrast, no filing defect with colour Doppler[a]	Echo density with viscid gelatinous features but without a solid component. Opacification with swirling contrast, no filling defect with colour Doppler[a]	Echo dense mass with margins and motion distinct from the atrial wall. Filling defect with colour Doppler[a], echo-free area with contrast
Thromboembolic risk	↑	↑↑	↑↑↑

[a]Low Nyquist limit, 25–35 cm/s.

Table 8 Imaging markers of cardioembolic risk

TTE	TOE	CMR	CCT
LA volumes	LAA emptying velocity SEC in LA, LAA	LA volumes	LA volumes
LA strain	Sludge/thrombus in LA or LAA	LA fibrosis	SEC in LA, LAA
SEC in LA	LAA non-chicken wing morphology	LA strain	LA or LAA thrombus
Thrombus in LA	PFO	LA 4D flow	LAA non-chicken wing morphology

associated with reduced LA function.[119–122] LA cardiopathy holds diagnostic[122] and prognostic significance for all-cause mortality and increased risk of AF development and cardioembolic events in CA.[118,122]

MR

LA dilation is an adaptive response to volume overload in patients with progressive MR.[123,124] Furthermore, enlarged LAVI identifies individuals at increased risk of mortality, independent of the severity of MR or AF.[125] The 2021 European Society of Cardiology (ESC)/European Association of Cardiothoracic Surgery (EACTS) Guidelines for the management of valvular heart diseases recommend early surgical mitral valve repair in low-risk asymptomatic patients with severe primary MR when LAVI ≥60 mL/m^2 or LA diameter ≥55 mm.[123] In addition to LA dilation, reduced LASr has been independently associated with all-cause mortality in patients with significant primary and secondary MR and has shown incremental prognostic value over LAVI and LV GLS.[126,127] LA fibrosis that occurs in the process of MR also reduces LASr.[128] The impact of mitral valve repair on the reversibility of LA fibrosis is currently investigated by LGE CMR (NCT05345730).[41] In atrial functional MR, which occurs most commonly in the setting of chronic HFpEF or AF, LA dilatation is deemed to be the main driver of MR through annular dilatation.[129] LA reverse remodelling after mitral valve repair is a favourable prognosticator but depends on several factors including pre-operative LAVI, MR severity, post-operative trans-mitral pressure gradient,[130] and intrinsic atrial cardiopathy. Recently, bi-leaflet prolapse was found to be associated with reduced LA function regardless of MR severity, suggesting a primary cardiopathy in these patients.[131]

MS

The pressure overload in MS promotes excessive dilatation of the LA with decreasing deformability, compliance, and contraction. In rheumatic MS, rheumatic atrial cardiopathy further exacerbates LA enlargement leading to one of the largest LAs observed in humans. The assessment of LA remodelling in MS includes LA size, EF, emptying fraction, PV flow patterns, LAA function, and LA deformation. From a clinical standpoint, LA compliance rather than the size is instrumental for mitigating pulmonary hypertension and increasing stroke volume downstream, whereby modulating symptoms in MS.[132] LA reservoir function, quantified by longitudinal strain, reflects LA compliance and is a function of pure MS in young subjects. Of note, concomitantly reduced LV compliance would affect LA compliance, LASr, conduit, and pump strain in the elderly[75] which is typical for degenerative MS with mitral annular calcification. LA dilatation and reduced LASr predict symptoms, hospitalizations, valve intervention, recurrence of functional tricuspid regurgitation after tricuspid valvuloplasty,

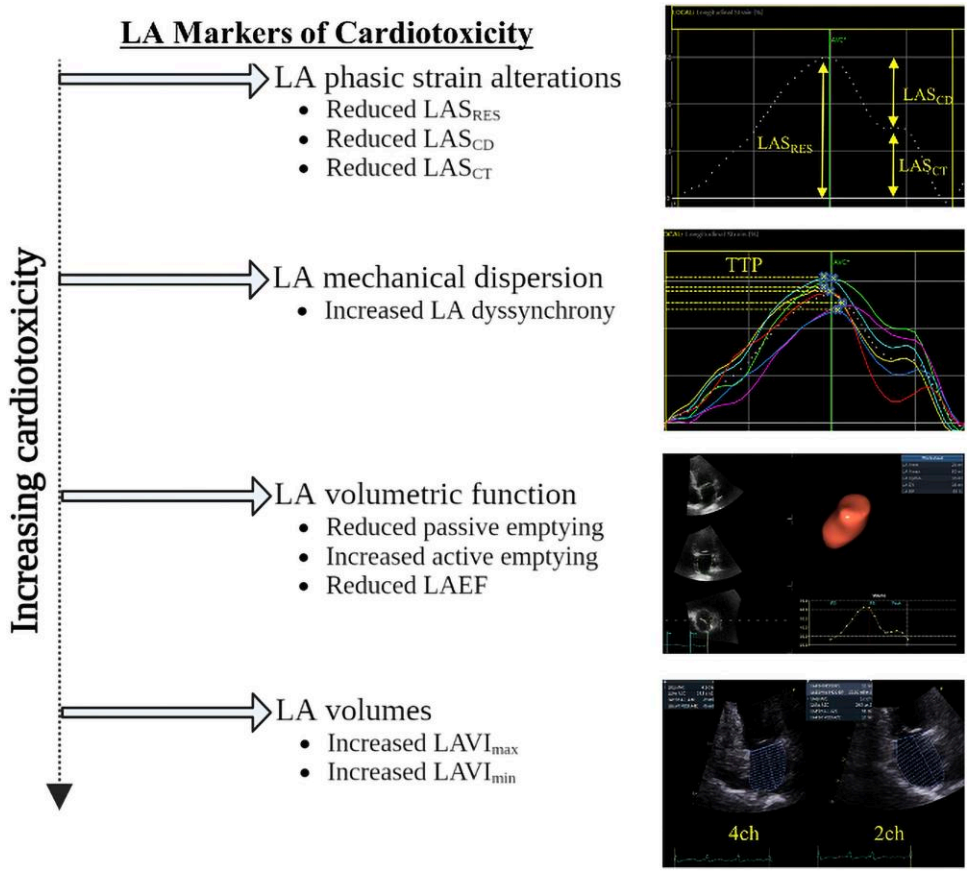

Figure 18 LA markers of cardiotoxicity.

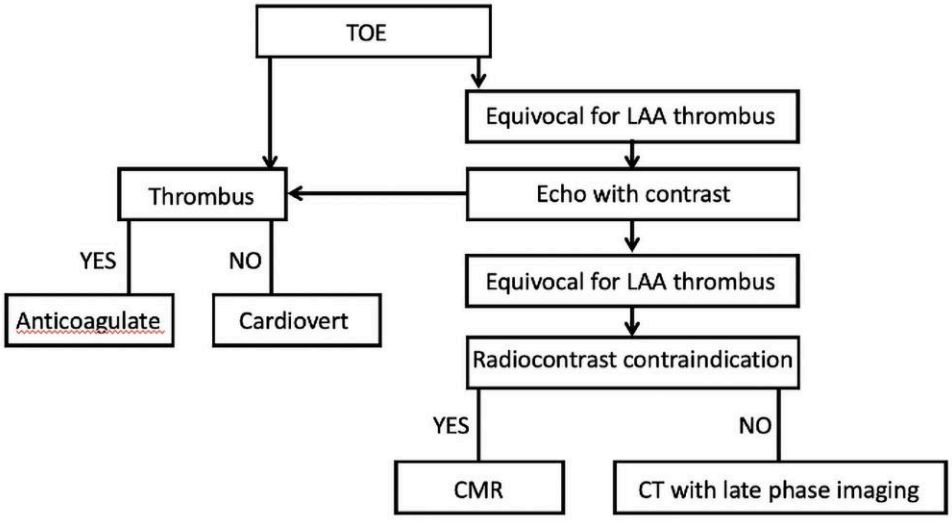

Figure 19 Imaging algorithm for direct-current cardioversion.

and AF and thromboembolic complications.[133–140] Anticoagulation with vitamin K antagonists should be considered if LAVI exceeds 60 mL/m^2 in patients with rheumatic MS even in sinus rhythm according to the 2021 ESC/EACTS Guidelines for the management of valvular heart disease.[123] Importantly, LASr and LA compliance were shown to improve following balloon mitral valvuloplasty, and this improvement translates into functional capacity.[141,142] Similarly, LAA contraction was shown to improve after balloon mitral valvuloplasty.[143]

AF

Atrial contraction is abolished during AF. Atrial volume increases, while LA reservoir function decreases (*Figure 16*). LA remodelling and fibrosis

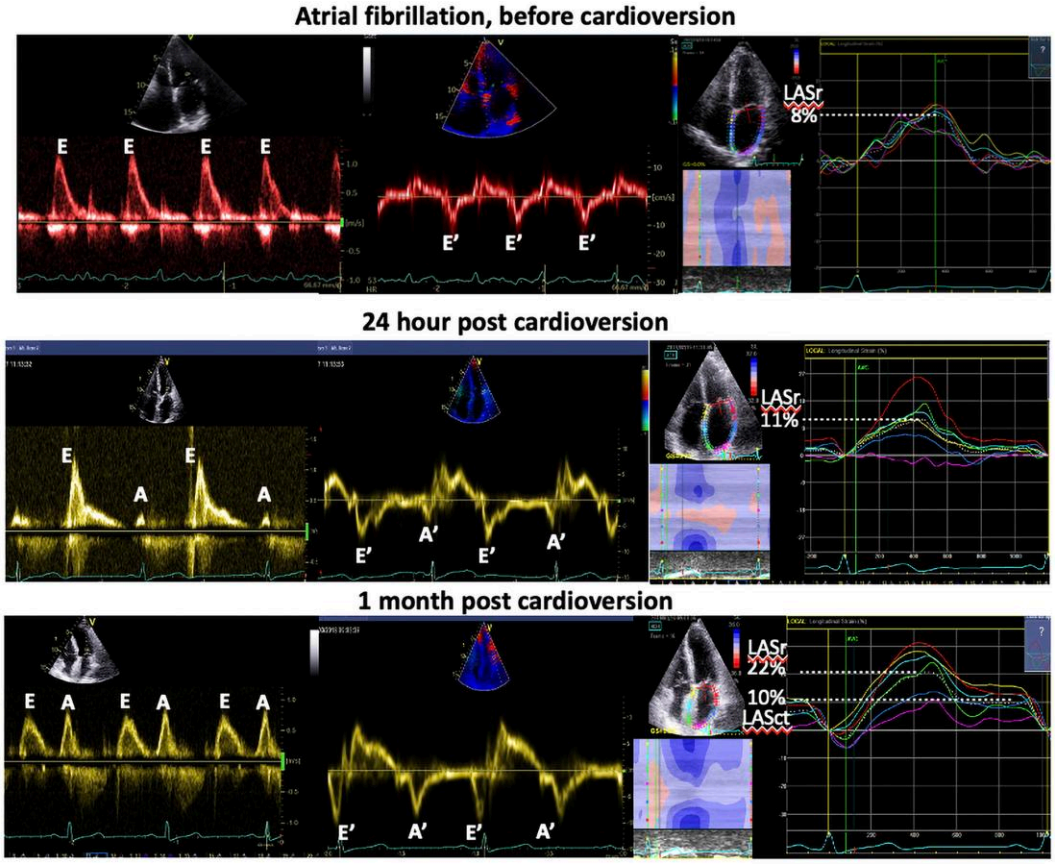

Figure 20 LA function before, early after, and late after cardioversion. Note the regeneration of LA contraction (A, a′, LASct).

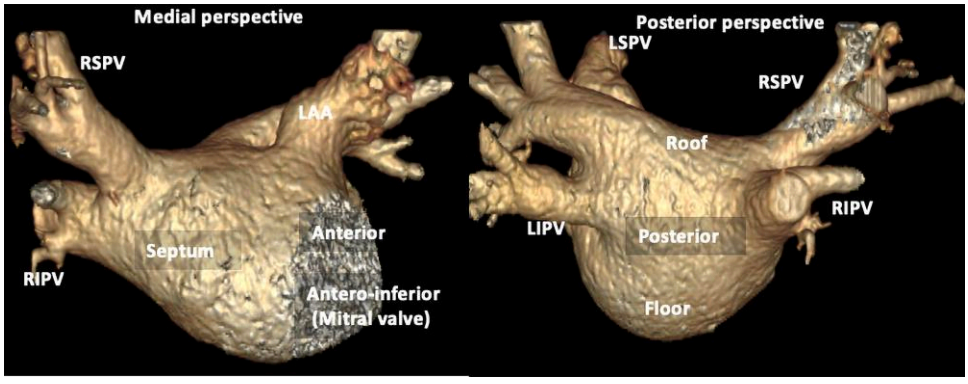

Figure 21 Demonstration of different parts of LA from a 3D volume-rendered reconstruction by contrast CCT performed for the assessment of PVs prior to PV isolation.

contribute to the perpetuation of AF.[144,145] Dilatation of the LA predicts the development of AF in the elderly and its predictive value is incremental to linear measurements.[146] Likewise, LA enlargement predicts AF recurrence after radiofrequency ablation or cardioversion.[147] Total atrial conduction time which is the time interval from the onset of P wave to atrial contraction (tissue Doppler *a'*) has been considered as a marker of LA fibrosis and shown to predict AF recurrence in patients following rhythm control strategy.[148]

LASr is an early marker of altered structure and impaired function.[149] In AF, measurements are averaged from five consecutive cycles. Only LASr can be computed during AF.[24,25] LASr predicted AF development in patients at risk in the general population,[150] in patients undergoing cardiac surgery, and in patients after a first stroke while in sinus rhythm.[133,151,152] Hence, LASr has the potential to improve risk stratification for AF development and monitoring strategies.[153] From a prognostic standpoint, improvement in LASr is associated with a higher rate of sinus rhythm maintenance after cardioversion or ablation.[154–156] Furthermore, an inverse relationship has been shown between LA strain and the extent of fibrosis measured by LGE CMR.[157] Of note, for diagnostic and prognostic purposes, in other diseases such as HFpEF and MR, LA enlargement and LASr should be interpreted with caution in the presence of AF.

Several studies showed that larger amounts of epicardial fat were associated with an increased risk of AF.[158] Moreover, Wong *et al.*[159] showed a more robust association of AF with epicardial fat as compared to abdominal or overall adiposity.

Thromboembolism

Visualization of thrombus

Thrombi can be found free-floating or attached to the LA wall, in-transit across the patent foramen ovale (PFO), on prosthetic materials (valves, occluders), or in the LAA. LAA is the most common location of thrombi (98%) in non-valvular AF because of stasis in the blinded pouch.[160,161]

TOE is the most frequently used tool to diagnose thrombus (sensitivity 93–100% and specificity 99%) in the LAA.[162] The use of ultrasound contrast agents improves the diagnostic accuracy of TOE for detecting thrombus (*Figure 17*).[163] False-positive results are frequently due to the misdiagnosis of pectinate muscles as thrombi. Differential diagnosis also includes masses with a potential for embolization such as fibroelastomas, tumours, or vegetations. Contrast-enhanced CMR is the method of choice to make the differential diagnosis of intracardiac masses.[164]

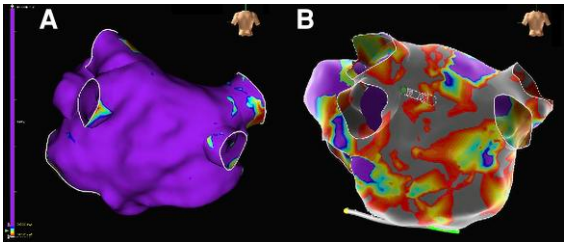

Figure 22 Electro-anatomical colour-coded voltage map (violet voltage >0.5 mV). (*A*) Normal voltage of the posterior wall. (*B*) Low-voltage areas and scar (grey colour) in native atrial cardiopathy.

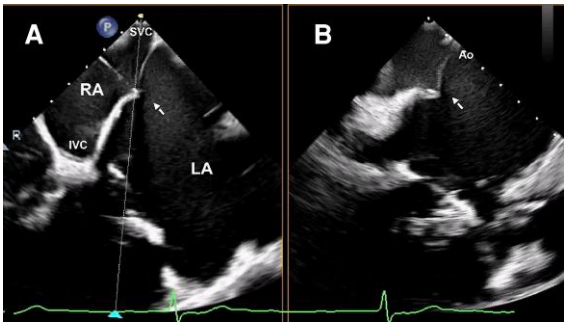

Figure 24 Trans-septal access with 3D ICE catheter using 2D X-plane imaging. A) the inter-atrial septum (IAS) is imaged in the superior and inferior orientation with the ICE catheter tip retroflexed. B) X-plane showing the anterior (Ao) and posterior. SVC- Superior vena cava; IVC = Inferior Vena Cava.

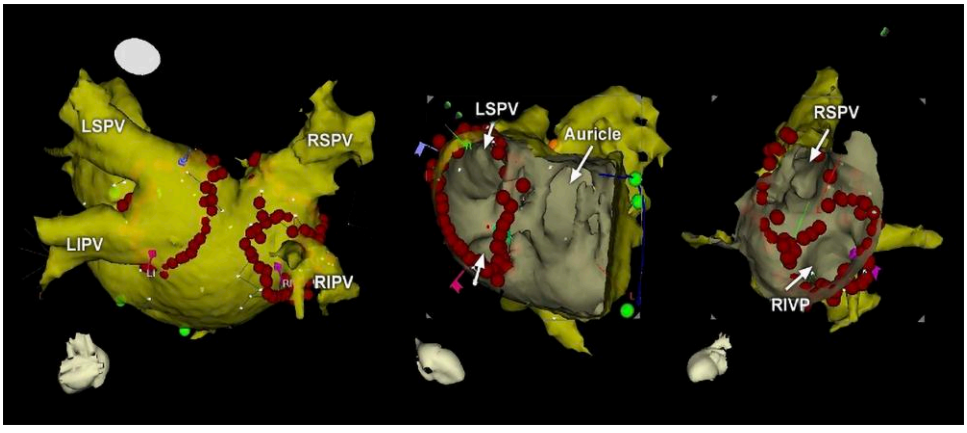

Figure 23 Integration of pre-acquired CCT reconstruction with electro-anatomical map used to guide PV isolation. The circle tags indicate radiofrequency energy delivery sites at the PV ostia. LSPV, left superior PV; LIPV, left inferior PV; RSPV, right superior PV; RIPV, right inferior PV.

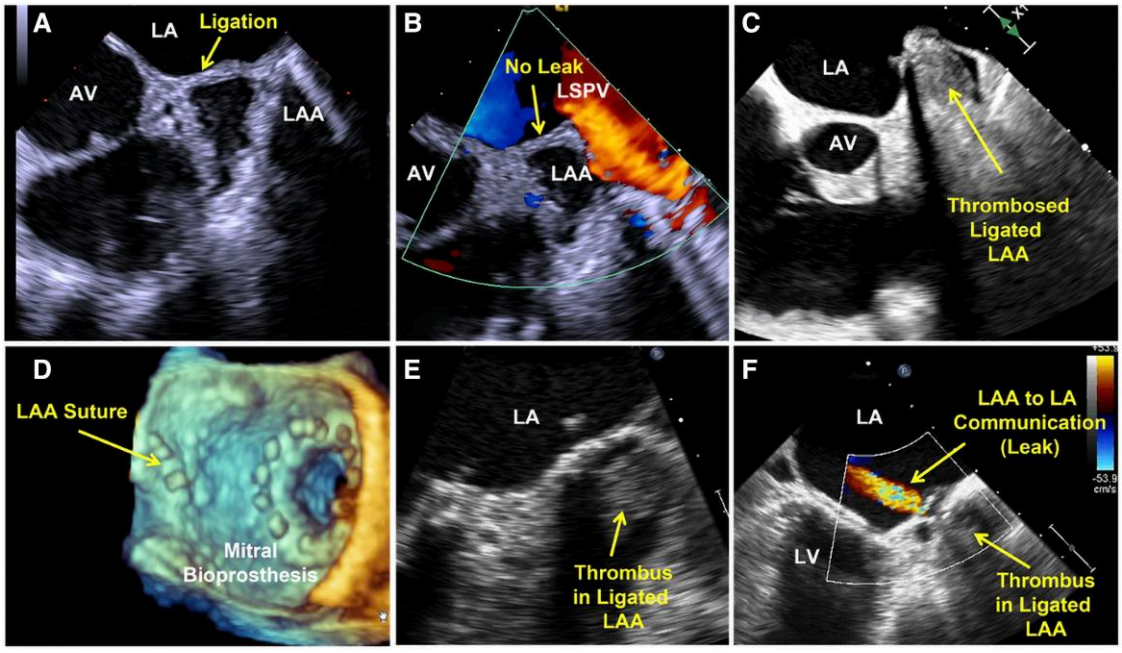

Figure 25 Surgically ligated LAA. A,B) surgically ligated LAA with no residual leak, C) subsequent tissue ingrowth and thrombus formation inside the ligated LAA, D) suture line, E) thrombus inside an incompletely ligated LAA, F) the residual LAA to LA communication.

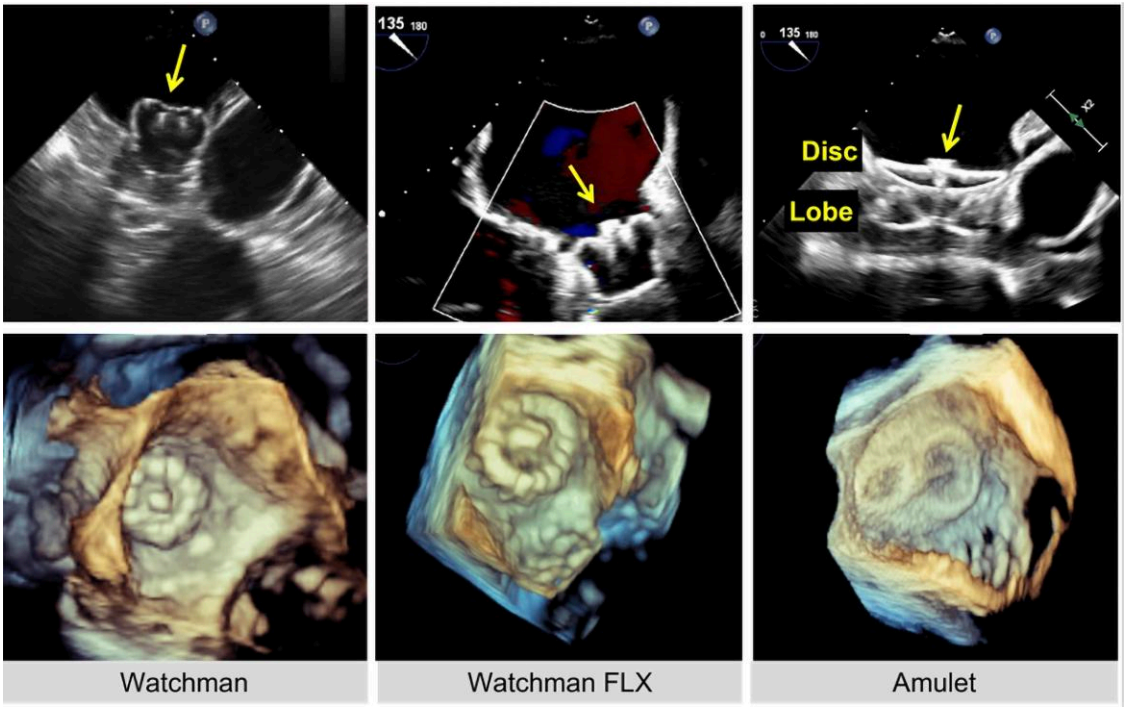

Figure 26 LAA closure devices correctly deployed seen by 2D saggital and 3D en face views.

CCT and CMR with dedicated protocols that ensure full replenishment of the LAA by contrast (see CMR and CCT) are also highly diagnostic (99%) for detecting LAA thrombus (*Figure 12*).[53,165–168] However, CCT and CMR are less well studied for detecting circulatory stasis within the LAA.[166,168]

Cardioembolic risk assessment

Imaging provides comprehensive information about thromboembolic risk: mitral valve prostheses, PFO, atrial septal defect (ASD), LA dilatation, loss of LA contraction, thrombus, and spontaneous echocardiographic contrast (SEC) are risk factors that are detected by imaging, for cardioembolic events. SEC is a marker of stagnation associated with low flow velocities in the LAA (<20 cm/s) and a precursor of thrombus.[169] The presence of dense SEC is a strong risk factor for thromboembolic events.[170–172] In terms of severity, SEC is graded semi-quantitatively[173] (*Table 7*). On the other hand, sludge gives the impression of impending thrombus and is associated with thromboembolism and all-cause mortality.[174] Following cardioversion, LAA and LA mechanical contractile dysfunction or 'stunning' develops in 38–80% of cases, with the formation of SEC.[175] Importantly, SEC does not disappear with anticoagulation.

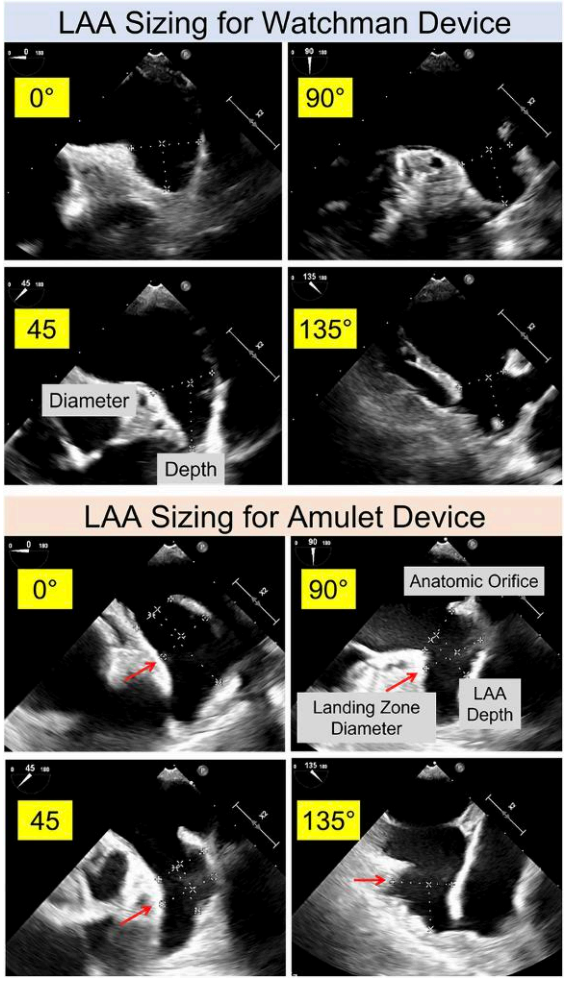

Figure 27 LAA Sizing by 2D TOE at 4 angles, 45 degrees apart (0, 45, 90 and 135°).

The size of LAA (>34 cm^3), the number of lobes ≥3, a large 8non-chicken wing (cauliflower in particular) morphology, and low-velocity flow are considered risk factors for thrombus formation.[176–178] The risk of thrombus development in the LAA increases with velocities ≤55 cm/s.[176,177] Emptying velocity <20 cm/s is specifically associated with LAA thrombus formation.[32] The ratio of LVEF/LAVI <1.5 showed 100% sensitivity for predicting the presence of LAA thrombus in patients with non-valvular AF.[179,180]

AF associated with MS, HCM, CA, or CHA_2DS_2-VA score >1 is an indication of anticoagulation[181] (vitamin K antagonists for moderate-to-severe MS). However, the temporal dissociation between the AF episodes and embolic stroke,[182,183] rhythm control strategies that failed to reduce the risk of stroke, suggested the possible impact of LA cardiopathy and metabolic factors to thrombogenic substrate.[184] Furthermore, LA dilatation[185,186] reduced deformation,[187–189] fibrosis,[190,191] and other atrial cardiopathy markers were shown to be associated with cardioembolic risk regardless of AF.[192–194] LA fibrosis and LA strain were also shown to provide incremental risk prediction over CHA_2DS_2-VASc score and LA volume.[187,195] The extent of LA fibrosis on LGE CMR was associated with LAA thrombus, stroke, and incident AF.[196,197] Likewise, patients with reduced LA strain had a higher incidence of LAA dysfunction and LAA thrombus in non-valvular AF.[198] Ongoing studies are further exploring the relationship between atrial fibrosis and stroke (NCT03830983).[199] Various markers of cardioembolic risk can be obtained from different imaging modalities (*Table 8*).

Chemotherapy-related cardiotoxicity

This section mainly focuses on the most commonly encountered anthracycline and trastuzumab toxicity. LA dilation was reported as an indicator of cardiotoxicity.[200–205] Alterations in LA function without changes in volume,[206–209] reduced passive emptying with increased active emptying,[205,206] and reduced LA emptying fraction by 3DE[210] and CMR[202] have been reported. Also, reduced LASr and conduit strain,[206–208] decreased LA contractile strain, and prolonged mechanical dispersion have been noted

Advice table 5 Multi-modality imaging of LA and LAA for disease-oriented purposes

Heart failure	
Assessment of LASr is advised as an adjunct to EACVI/ASE criteria of DD.[70,73]	
Both LASr and LAVI quantification is advised whenever HFpEF is suspected or established.	
Quantification of LASr and LAVI is advised as part of the assessment of functional and structural cardiac abnormality (previously designated as Stage B HF).	
Ischaemic heart disease	
Assessment of LAVI and LASr may be appropriate for risk stratification in acute and chronic ischaemic heart disease independently of LV ejection fraction.	
Athlete's heart	
It is advised to assess LA enlargement as an adaptative mechanism in athletes.	
LA size or strain is not suitable for differentiating adaptive from pathological remodelling in athletes.	
Hypertrophic cardiomyopathy	
Assessment of LA cardiopathy (dilatation, dysfunction, and fibrosis) is integral to the evaluation of HCM as an adjunct to diagnosis and prognostication.	

Cardiac amyloidosis

Assessment of LA cardiopathy (dilatation, dysfunction, and fibrosis) is advised for the diagnosis and prognostication of CA

Identification of atrial electromechanical dissociation is a distinct clinical phenotype indicating poor prognosis in CA

Mitral regurgitation

In primary MR, it is appropriate to evaluate LA size for making decision about mitral valve intervention.

It is appropriate to evaluate LA dilatation, annular dilatation, and altered annular contraction for the diagnosis of atrial functional MR.

Mitral stenosis

Quantification of LA function and remodelling complements the haemodynamic assessment of MS and prognostication.

Atrial fibrillation

Assessment of LAVI and LASr is advised to improve prediction of the risk of AF development, persistence, and recurrence during sinus rhythm in subjects with CHA_2DS_2-VA score >1 (excluding gender), moderate-to-severe rheumatic MS, HCM, and CA.

Cut-offs for abnormal LA size and function are not valid in the presence of AF for diagnostic and prognostic purposes.

Thromboembolism

The use of ultrasound contrast agents is advised to increase the accuracy of TOE as needed to rule out cardiac thrombus.

TOE and delayed contrast imaging with CCT or CMR with inversion time myocardial delayed enhancement are appropriate to rule out LA/LAA thrombus.[181,216]

Assessment of LA cardiopathy by volume, strain, and LAA dysfunction is advised as risk modifiers during sinus rhythm.

Anticoagulation within the therapeutic range should not be interrupted before TOE.

LA cardiopathy alone is not considered a valid argument for anticoagulation.

(*Figure 18*).[211] LA function parameters are sensitive markers and usually precede LA volume increase. They correlate with LV DD and AF generation. Of note, Ibrutinib-related AF is a well-known cardiotoxic complication for which LASr was found as an important predictor.[212,213] Cut-offs for LA cardiotoxicity are not standardized, with studies using absolute LASr <35% or <10th percentile, ≥10–15% reduction from baseline or comparison to controls. Yet, the prognostic utility of LASr in predicting cardiotoxicity remains debatable.[214,215]

Peri-procedural imaging of LA and LAA for outcome optimization

Cardioversion

The Assessment of Cardioversion Using TOE (ACUTE) multi-centre trial was the first randomized prospective study that introduced TOE-guided cardioversion into clinical practice.[217,218] Today, the TOE-guided approach is the common strategy when there is a sub-therapeutic or interrupted anticoagulation over the last 3 weeks to expedite cardioversion[181,219–222] (*Figure 19*). Atrial stunning is maximum immediately after cardioversion and improves typically over 4 weeks (*Figure 20*).[223] It is important not to stop the anticoagulation during atrial stunning. Of note, full recovery of mechanical function may extend beyond 3 months in almost 50% of the patients, depending on the duration of AF, atrial size, and structural heart disease.[224]

Peri-AF ablation

Depending on experience and resources, CCT and ICE are used in clinical practice for visualizing LA/LAA thrombus before catheter ablation as alternatives to TOE. The following groups are considered high risk for thromboembolic complications: (i) patients with CHA_2DS_2-VA >1 but have not received therapeutic anticoagulation during the last 3 weeks; (ii) patients having CA, HCM, and rheumatic moderate-to-severe MS, despite therapeutic anticoagulation within the last 3 weeks; and (3) patients with a history of thrombus despite therapeutic anticoagulation.[181,225] Imaging should be close in time to the procedure, ideally within 48 h. The anatomic modelling of PVs before AF ablation may impact the ablation approach and can be accurately performed by CCT or CMR with contrast.[216,225,226] Of note, there is less data with CMR for PV modelling. Therefore, CCT is more frequently used than CMR for clinical practice (*Figure 21*). Imaging for PV stenosis post-ablation is only required if patients are symptomatic.[225]

Electroanatomic mapping (EAM) systems serve to obtain real-time anatomical information from the LA, LAA, and PVs and identify low-voltage areas that may be additional targets for AF ablation beyond PV isolation (*Figure 22*).[227,228] Preprocedural CCT images loaded and merged with the real-time mapping system can facilitate anatomic reconstruction, pre-acquired delayed enhancement CMR sequences may assist with the identification of scar extent and location[39,228–230] (*Figure 23*). Although integration of pre-acquired CCT or CMR images was thought to decrease the fluoroscopy duration, previous randomized studies and a new meta-analysis demonstrated that integration of pre-acquired CCT or CMR images does not improve outcomes from AF ablation.[216,225,226,231]

Although among patients with AF undergoing catheter ablation, fibrosis estimated by delayed enhancement was found to be associated with the likelihood of recurrent arrhythmia in the Determinant of Successful Radiofrequency Catheter Ablation of Atrial Fibrillation (DECAAF) study,[232] the DECAAF-2 study did not demonstrate the benefit of adding CMR-guided fibrosis ablation to PV isolation for preventing atrial arrhythmia recurrence.[39] CMR may allow visualization of completeness of post-ablation lesions which is relevant for the recurrence of AF.[233,234]

CCT is the preferred imaging modality to assess PV stenosis after PV isolation.[235]

Lately, ICE has become a useful guide for AF ablation procedures. ICE enables visualization of PV ostia, the position of catheters and guides trans-septal puncture, thereby increasing the safety of the procedure (*Figure 24*).[236–238]

Imaging is key to diagnosing complications of the procedures. Pericardial effusion is the most common complication of AF ablation (0.4–1.3%).[225] Echocardiography should be readily available to make the diagnosis. Echocardiography is also the first step for assessing when valvular damage is suspected. Thrombotic complications and PV stenosis are diagnosed with CCT or CMR with contrast while atrio-oesophageal fistula is best diagnosed by chest CT with contrast.[216,239,240] Further work-up for the management of complications is described in the European Heart Rhythm Association (EHRA)/EACVI document on cardiac imaging in electrophysiology.[216]

LAA closure

It is advised to exclude LAA thrombus before percutaneous LAA closure in every patient. Surgical exclusion requires less guidance with

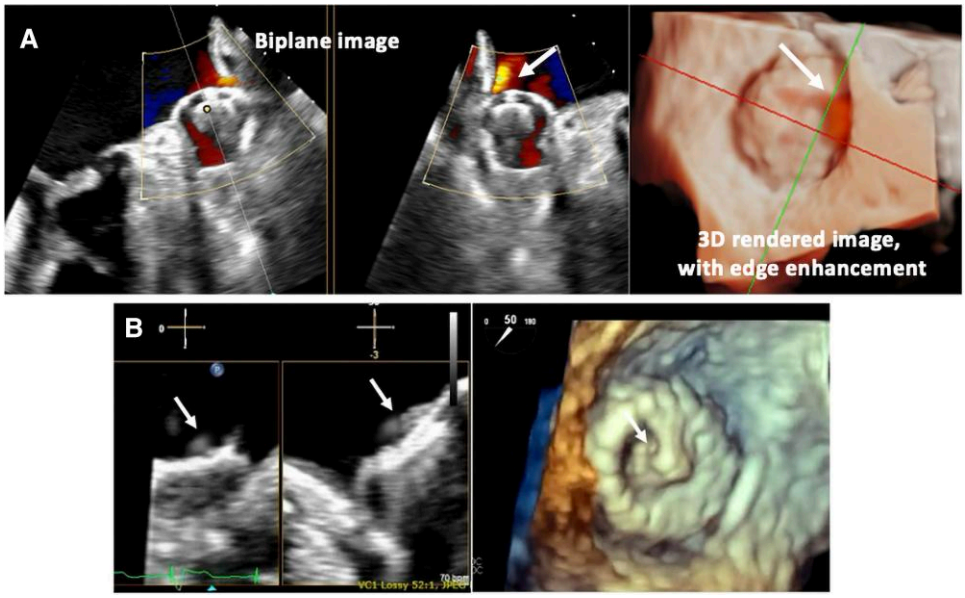

Figure 28 A) Peri-device leak by color Doppler (arrows), B) Thrombus on the occluder (arrows).

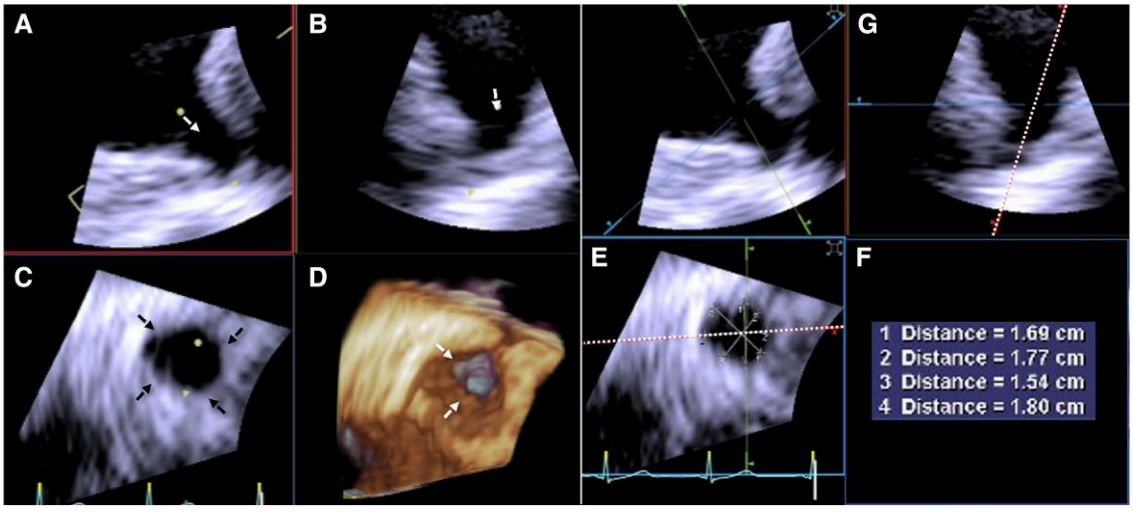

Figure 29 Imaging the LAA with the AcuNav 3D ICE catheter in the LA. (*A*, *B*) Long-axis orientations equivalent to 45 and 135° TOE views, respectively. (*C*) Short-axis view of the LAA ostia. These 2D multiplanar reconstructions are generated from the volume data shown in D. (*E*) Measurements of the ostial size in the four standard orientations of conventional TOE guidance. (*F*) Additional measurements obtained from E. (*G*) Depth of LAA (dotted line).

imaging, but post-surgical evaluation is important because it may be incomplete and may paradoxically increase the risk of thromboembolism[241] (*Figure 25A–F*). Various transcatheter closure devices are in use with specific appearances (*Figure 26*).[242–244] Measurements for device sizing are performed either by TOE or CCT. Device sizing aims to determine the maximum landing zone diameter at the level of the left circumflex artery (*Figure 27*). Sizing by CCT offers higher spatial resolution and tends to be 2–3 mm larger than TOE.[245] CCT can also be useful for selecting trans-septal puncture site.[246] Intraprocedural guidance utilizes a combination of fluoroscopy with either TOE or ICE. The goal is to achieve a complete occlusion of the LAA orifice without peri-device leak (PDL). The size of a PDL is measured at its narrowest diameter (vena contracta) by colour Doppler using a Nyquist limit of ~35 cm/s. Recent studies have shown that irrespective of the size, patients with PDLs have a higher incidence of thromboembolic complications compared with those without PDL.[247,248] A device surveillance at 45–90

Advice table 6 Peri-procedural use of multi-modality imaging

Cardioversion	
Imaging to rule out cardiac thrombus before cardioversion is advised in indications defined by the 2024 ESC guidelines for the management of AF[a].[181]	
Transcatheter and surgical procedures	
Cardiac imaging prior to AF ablation in high-risk patients may be useful (see text).	
Guidance with TOE or ICE is advised for transcatheter LAA occlusion.	
CCT is the preferred modality for assessing PV patterns before AF ablation and PV stenosis post-ablation, in symptomatic patients.	
Guidance with ICE increases the safety and decreases the duration of AF ablation.[237,238]	
Echocardiography should be readily available in the catheter laboratory.	
Chest CT with contrast is advised when there is suspicion of atrio-oesophageal fistula after AF ablation.	
The utility of assessing LA wall fibrosis with CMR before and after AF ablation is uncertain.	
TOE should be avoided if there is suspicion of atrio-oesophageal fistula.	

[a](i) To expedite cardioversion in non-anticoagulated subjects with AF ≥24 h and CHA_2DS_2-VA >1, (ii) if anticoagulation has been suboptimal within the last 3 weeks without interruption, and (iii) after 4 weeks of anticoagulation if a thrombus was initially detected.

days by TOE is advised to verify device stability, erosion, and complete occlusion without PDL and to rule out thrombus that is associated with unfavourable outcomes[245] (*Figure 28*). Patients with PDLs may either require anticoagulation or undergo additional transcatheter closure procedures.

ICE is frequently used during LAA device closure.[249] LAA views are optimally obtained when the ICE catheter is positioned in the right ventricle or the pulmonary artery. However, invasive nature and high costs of the technique limit its use (*Figure 29*).

Future perspectives

Developments in molecular imaging are promising to explore the inflammation and fibrotic process associated with atrial cardiopathy. Computational fluid dynamics simulations enable comprehensive blood flow pattern analysis in the LA, LAA, and PVs helping to explore the thrombogenic milieu.[250] Nevertheless, some simple but important gaps in evidence restrict the widespread clinical use of imaging for the assessment of LA cardiopathy. LA cardiopathy for risk stratification in patients having severe aortic stenosis,[251] the impact of assessing LA remodelling on outcomes, diagnostic and prognostic cut-offs of LA remodelling specific to diseases, and imaging modalities are awaited.

Conclusions

Consistent evidence and uniform expert consensus favour assessing LA cardiopathy and LAA by multi-modality imaging as an indispensable adjunct to patient management. The major gaps in evidence include the demonstration of the game-changing impact of multi-modality imaging for improving the outcomes. Further evidence from randomized studies is awaited to integrate multi-modality imaging of LA and LAA into clinical decision-making algorithms of the guidelines for patient management.

Acknowledgements

We would like to thank Dr. Benay Ozbay for her devoted help in the redaction of the manuscript.

Conflict of interest: L.E.S., member of the editorial board—*European Heart Journal Cardiovascular Imaging*. F.F.F., speaker fee from Phillips. G.P., honorarium as speaker/consultant and/or institutional research grants from GE HealthCare, Bracco, HeartFlow, Novartis, Alexion, and Menarini; member of the editorial board—*European Heart Journal Cardiovascular Imaging*. B.L.M.G., consultant Bristol Myers Squibb and Novartis; member of the editorial board—*European Heart Journal Cardiovascular Imaging*. D.M., member of the editorial board—*European Heart Journal Cardiovascular Imaging*. T.E., none. B.C., none. B.A.P., none. A.K., research grant Kiniksa and Cardiol Therapeutics and scientific advisory board for Kiniksa, Cardiol Therapeutics, and Pfizer. T.H.M., none. M.C., none. M.S., speakers bureau (Abbott, Boston Scientific, Medtronic). L.T., speaker fees from Pfizer, Sanofi, and Janssen-Cilag; honoraria from Bayer. N.A.M., speaker fees from GE HealthCare, Philips Ultrasound, and Abbott Vascular; research grants from Pfizer, Alnylam, AstraZeneca, Edwards Lifesciences, and Pie Medical Imaging. R.F-C., none. T.P., none. M.F., consultancy/advisory boards for Alnylam, Alexion/Caelum Biosciences, AstraZeneca, BridgeBio/Eidos, Prothena, Attralus, Intellia Therapeutics, Ionis Pharmaceuticals, Cardior, Lexeo Therapeutics, Janssen Pharmaceuticals, Prothena, Pfizer, Novo Nordisk, Bayer, and MyCardium; research grants from Alnylam, BridgeBio, AstraZeneca, and Pfizer; salary from the British Heart Foundation Intermediate Fellowship; share options in Lexeo Therapeutics and shares in MyCardium. A.L.G., none. S.E.P., consultancy, Circle Cardiovascular Imaging, Inc., Calgary, Alberta, Canada. S.M-E., none. M.S.B., speaker fee from Cleerly. M.A.V. (all support to the institution and not to self), research support from Philips, GE HealthCare, Siemens Healthineers, Biosense Webster, Johnson & Johnson, Abbott, and Medtronic; speaker honorarium from Siemens Healthineers, Johnson & Johnson, Philips, Abbott, and Medtronic. M.G., none. P.P., honoraria and consultation fees from Medtronic, Boston Scientific, Abbott, Biotronik, and Biosense Webster. H.C., Founder and shareholder at inHEART Medical. I.S., speaker or advisory board fees from Novartis, AstraZeneca, Pfizer, Takeda, Servier, Boehringer Ingelheim, and Janssen. E.D., research facilities and a grant from GE HealthCare and Abbott Structural; consulting fees from Pfizer, Alnylam, and Bristol Myers Squibb; member of the editorial board—*European Heart Journal Cardiovascular Imaging*.

Data availability

The data underlying this article are provided by the EACVI by permission. Data will be shared on request to the corresponding author with permission of the EACVI.

References

1. Goette A, Kalman JM, Aguinaga L, Akar J, Cabrera JA, Chen SA *et al.* EHRA/HRS/APHRS/SOLAECE expert consensus on atrial cardiomyopathies: definition, characterization, and clinical implication. *Europace* 2016;**18**:1455–90.
2. Ho SY, Cabrera JA, Sanchez-Quintana D. Left atrial anatomy revisited. *Circ Arrhythm Electrophysiol* 2012;**5**:220–8.
3. Delgado V, Di Biase L, Leung M, Romero J, Tops LF, Casadei B *et al.* Structure and function of the left atrium and left atrial appendage: AF and stroke implications. *J Am Coll Cardiol* 2017;**70**:3157–72.
4. Beigel R, Wunderlich NC, Ho SY, Arsanjani R, Siegel RJ. The left atrial appendage: anatomy, function, and noninvasive evaluation. *JACC Cardiovasc Imaging* 2014;**7**:1251–65.
5. Lang RM, Badano LP, Mor-Avi V, Afilalo J, Armstrong A, Ernande L *et al.* Recommendations for cardiac chamber quantification by echocardiography in adults: an update from the American Society of Echocardiography and the European Association of Cardiovascular Imaging. *J Am Soc Echocardiogr* 2015;**28**:1–39.e14.
6. Venkateshvaran A, Tureli HO, Faxén UL, Lund LH, Tossavainen E, Lindqvist P. Left atrial reservoir strain improves diagnostic accuracy of the 2016 ASE/EACVI diastolic

algorithm in patients with preserved left ventricular ejection fraction: insights from the KARUM haemodynamic database. *Eur Heart J Cardiovasc Imaging* 2022;**23**:1157–68.
7. Davis CA, Rembert JC, Greenfield JC. Compliance of left atrium with and without left atrium appendage. *Am J Physiol* 1990;**259**:H1006–8.
8. Blume GG, Mcleod CJ, Barnes ME, Seward JB, Pellikka PA, Bastiansen PM *et al.* Left atrial function: physiology, assessment, and clinical implications. *Eur J Echocardiogr* 2011; **12**:421–30.
9. Nunes MCP, Handschumacher MD, Levine RA, Barbosa MM, Carvalho VT, Esteves WA *et al.* Role of LA shape in predicting embolic cerebrovascular events in mitral stenosis: mechanistic insights from 3D echocardiography. *JACC Cardiovasc Imaging* 2014;**7**: 453–61.
10. Badano LP, Pezzutto N, Marinigh R, Cinello M, Nucifora G, Pavoni D *et al.* How many patients would be misclassified using M-mode and two-dimensional estimates of left atrial size instead of left atrial volume? A three-dimensional echocardiographic study. *J Cardiovasc Med (Hagerstown)* 2008;**9**:476–84.
11. Elliott PM, Anastasakis A, Borger MA, Borggrefe M, Cecchi F, Charron P *et al.* 2014 ESC guidelines on diagnosis and management of hypertrophic cardiomyopathy: the Task Force for the Diagnosis and Management of Hypertrophic Cardiomyopathy of the European Society of Cardiology (ESC). *Eur Heart J* 2014;**35**:2733–79.
12. Thomas L, Muraru D, Popescu BA, Sitges M, Rosca M, Pedrizzetti G *et al.* Evaluation of left atrial size and function: relevance for clinical practice. *J Am Soc Echocardiogr* 2020; **33**:934–52.
13. Badano LP, Miglioranza MH, Mihăilă S, Peluso D, Xhaxho J, Marra MP *et al.* Left atrial volumes and function by three-dimensional echocardiography: reference values, accuracy, reproducibility, and comparison with two-dimensional echocardiographic measurements. *Circ Cardiovasc Imaging* 2016;**9**:e004229.
14. Surkova E, Badano LP, Genovese D, Cavalli G, Lanera C, Bidviene J *et al.* Clinical and prognostic implications of methods and partition values used to assess left atrial volume by two-dimensional echocardiography. *J Am Soc Echocardiogr* 2017;**30**:1119–29.
15. Florescu DR, Badano LP, Tomaselli M, Torlasco C, Târtea GC, Bălşeanu TA *et al.* Automated left atrial volume measurement by two-dimensional speckle-tracking echocardiography: feasibility, accuracy, and reproducibility. *Eur Heart J Cardiovasc Imaging* 2021;**23**:85–94.
16. Mor-Avi V, Yodwut C, Jenkins C, Kühl H, Nesser H-J, Marwick TH *et al.* Real-time 3D echocardiographic quantification of left atrial volume: multicenter study for validation with CMR. *JACC Cardiovasc Imaging* 2012;**5**:769–77.
17. Iwataki M, Takeuchi M, Otani K, Kuwaki H, Haruki N, Yoshitani H *et al.* Measurement of left atrial volume from transthoracic three-dimensional echocardiographic datasets using the biplane Simpson's technique. *J Am Soc Echocardiogr* 2012;**25**:1319–26.
18. Singh A, Carvalho Singulane C, Miyoshi T, Prado AD, Addetia K, Bellino M *et al.* Normal values of left atrial size and function and the impact of age: results of the World Alliance Societies of Echocardiography Study. *J Am Soc Echocardiogr* 2022;**35**:154–64.e3.
19. Sugimoto T, Robinet S, Dulgheru R, Bernard A, Ilardi F, Contu L *et al.* Echocardiographic reference ranges for normal left atrial function parameters: results from the EACVI NORRE study. *Eur Heart J Cardiovasc Imaging* 2018;**19**:630–8.
20. Motoc A, Roosens B, Scheirlynck E, Tanaka K, Luchian ML, Magne J *et al.* Feasibility and reproducibility of left atrium measurements using different three-dimensional echocardiographic modalities. *Diagnostics (Basel)* 2020;**10**:1043.
21. Medvedofsky D, Mor-Avi V, Amzulescu M, Fernández-Golfín C, Hinojar R, Monaghan MJ *et al.* Three-dimensional echocardiographic quantification of the left-heart chambers using an automated adaptive analytics algorithm: multicentre validation study. *Eur Heart J Cardiovasc Imaging* 2018;**19**:47–58.
22. Kou S, Caballero L, Dulgheru R, Voilliot D, De Sousa C, Kacharava G *et al.* Echocardiographic reference ranges for normal cardiac chamber size: results from the NORRE study. *Eur Heart J Cardiovasc Imaging* 2014;**15**:680–90.
23. Voigt J-U, Mălăescu G-G, Haugaa K, Badano L. How to do LA strain. *Eur Heart J Cardiovasc Imaging* 2020;**21**:715–7.
24. Badano LP, Kolias TJ, Muraru D, Abraham TP, Aurigemma G, Edvardsen T *et al.* Standardization of left atrial, right ventricular, and right atrial deformation imaging using two-dimensional speckle tracking echocardiography: a consensus document of the EACVI/ASE/Industry Task Force to standardize deformation imaging. *Eur Heart J Cardiovasc Imaging* 2018;**19**:591–600.
25. Cameli M, Miglioranza MH, Magne J, Mandoli GE, Benfari G, Ancona R *et al.* Multicentric atrial strain comparison between two different modalities: MASCOT HIT study. *Diagnostics (Basel)* 2020;**10**:946.
26. Pathan F, D'Elia N, Nolan MT, Marwick TH, Negishi K. Normal ranges of left atrial strain by speckle-tracking echocardiography: a systematic review and meta-analysis. *J Am Soc Echocardiogr* 2017;**30**:59–70.e8.
27. Nyberg J, Jakobsen EO, Østvik A, Holte E, Stølen S, Lovstakken L *et al.* Echocardiographic reference ranges of global longitudinal strain for all cardiac chambers using guideline-directed dedicated views. *JACC Cardiovasc Imaging* 2023;**16**: 1516–31.
28. Kim D, Seo JH, Choi KH, Lee SH, Choi J-O, Jeon E-S *et al.* Prognostic implications of left atrial stiffness index in heart failure patients with preserved ejection fraction. *JACC Cardiovasc Imaging* 2023;**16**:435–45.
29. Pathan F, Hecht H, Narula J, Marwick TH. Roles of transesophageal echocardiography and cardiac computed tomography for evaluation of left atrial thrombus and associated pathology: a review and critical analysis. *JACC Cardiovasc Imaging* 2018;**11**: 616–27.
30. Fiore G, Gaspardone C, Ingallina G, Rizza V, Melillo F, Stella S *et al.* Accuracy and reliability of left atrial appendage morphology assessment by three-dimensional transesophageal echocardiographic glass rendering modality: a comparative study with computed tomography. *J Am Soc Echocardiogr* 2023;**36**:1083–91.
31. To ACY, Gabriel RS, Park M, Lowe BS, Curtin RJ, Sigurdsson G *et al.* Role of transesophageal echocardiography compared to computed tomography in evaluation of pulmonary vein ablation for atrial fibrillation (ROTEA study). *J Am Soc Echocardiogr* 2011; **24**:1046–55.
32. Agmon Y, Khandheria BK, Meissner I, Schwartz GL, Petterson TM, O'Fallon WM *et al.* Left atrial appendage flow velocities in subjects with normal left ventricular function. *Am J Cardiol* 2000;**86**:769–73.
33. Peters DC, Lamy J, Sinusas AJ, Baldassarre LA. Left atrial evaluation by cardiovascular magnetic resonance: sensitive and unique biomarkers. *Eur Heart J Cardiovasc Imaging* 2021;**23**:14–30.
34. Kawel-Boehm N, Hetzel SJ, Ambale-Venkatesh B, Captur G, Francois CJ, Jerosch-Herold M *et al.* Reference ranges ('normal values') for cardiovascular magnetic resonance (CMR) in adults and children: 2020 update. *J Cardiovasc Magn Reson* 2020; **22**:87.
35. Ginami G, Lòpez K, Mukherjee RK, Neji R, Munoz C, Roujol S *et al.* Non-contrast enhanced simultaneous 3D whole-heart bright-blood pulmonary veins visualization and black-blood quantification of atrial wall thickness. *Magn Reson Med* 2019;**81**:1066–79.
36. Kato R, Lickfett L, Meininger G, Dickfeld T, Wu R, Juang G *et al.* Pulmonary vein anatomy in patients undergoing catheter ablation of atrial fibrillation: lessons learned by use of magnetic resonance imaging. *Circulation* 2003;**107**:2004–10.
37. Dong J, Dickfeld T, Dalal D, Cheema A, Vasamreddy CR, Henrikson CA *et al.* Initial experience in the use of integrated electroanatomic mapping with three-dimensional MR/CT images to guide catheter ablation of atrial fibrillation. *J Cardiovasc Electrophysiol* 2006;**17**:459–66.
38. Pontecorboli G, Figueras I Ventura RM, Carlosena A, Benito E, Prat-Gonzales S, Padeletti L *et al.* Use of delayed-enhancement magnetic resonance imaging for fibrosis detection in the atria: a review. *Europace* 2017;**19**:180–9.
39. Marrouche NF, Wazni O, McGann C, Greene T, Dean JM, Dagher L *et al.* Effect of MRI-guided fibrosis ablation vs conventional catheter ablation on atrial arrhythmia recurrence in patients with persistent atrial fibrillation: the DECAAF II randomized clinical trial. *JAMA* 2022;**327**:2296–305.
40. Zghaib T, Quinaglia AC, Silva T, Ambale-Venkatesh B, Xie E, Ostovaneh MR *et al.* Association between left atrial late gadolinium enhancement and atrial fibrillation: the Multi-Ethnic Study of Atherosclerosis (MESA). *Radiol Cardiothorac Imaging* 2023; **5**:e220047.
41. El Mathari S, Kluin J, Hopman LHGA, Bhagirath P, Oudeman MAP, Vonk ABA *et al.* The role and implications of left atrial fibrosis in surgical mitral valve repair as assessed by CMR: the ALIVE study design and rationale. *Front Cardiovasc Med* 2023;**10**:1166703.
42. Di Bella G, Minutoli F, Madaffari A, Mazzeo A, Russo M, Donato R *et al.* Left atrial function in cardiac amyloidosis. *J Cardiovasc Med (Hagerstown)* 2016;**17**:113–21.
43. Chen J, Zhang H, Zhu D, Wang Y, Byanju S, Liao M. Cardiac MRI for detecting left atrial/left atrial appendage thrombus in patients with atrial fibrillation: meta-analysis and systematic review. *Herz* 2019;**44**:390–7.
44. Mahajan R, Kuklik P, Grover S, Brooks AG, Wong CX, Sanders P *et al.* Cardiovascular magnetic resonance of total and atrial pericardial adipose tissue: a validation study and development of a 3 dimensional pericardial adipose tissue model. *J Cardiovasc Magn Reson* 2013;**15**:73.
45. Chen J, Mei Z, Yang Y, Dai C, Wang Y, Zeng R *et al.* Epicardial adipose tissue is associated with higher recurrence risk after catheter ablation in atrial fibrillation patients: a systematic review and meta-analysis. *BMC Cardiovasc Disord* 2022;**22**:264.
46. Spartera M, Pessoa-Amorim G, Stracquadanio A, Von Ende A, Fletcher A, Manley P *et al.* Left atrial 4D flow cardiovascular magnetic resonance: a reproducibility study in sinus rhythm and atrial fibrillation. *J Cardiovasc Magn Reson* 2021;**23**:29.
47. Maceira AM, Cosín-Sales J, Roughton M, Prasad SK, Pennell DJ. Reference left atrial dimensions and volumes by steady state free precession cardiovascular magnetic resonance. *J Cardiovasc Magn Reson* 2010;**12**:65.
48. Yang W, Xu J, Zhu L, Zhang Q, Wang Y, Zhao S *et al.* Myocardial strain measurements derived from magnetic resonance feature-tracking: influence of sex, age, field strength, and vendor. *JACC Cardiovasc Imaging* 2024;**17**:364–79.
49. Föll D, Taeger S, Bode C, Jung B, Markl M. Age, gender, blood pressure, and ventricular geometry influence normal 3D blood flow characteristics in the left heart. *Eur Heart J Cardiovasc Imaging* 2013;**14**:366–73.
50. Pontone G, Andreini D, Bertella E, Petullà M, Russo E, Innocenti E *et al.* Comparison of cardiac computed tomography versus cardiac magnetic resonance for characterization of left atrium anatomy before radiofrequency catheter ablation of atrial fibrillation. *Int J Cardiol* 2015;**179**:114–21.

51. Andreini D, Pontone G, Mushtaq S, Conte E, Perchinunno M, Guglielmo M *et al.* Atrial fibrillation: diagnostic accuracy of coronary CT angiography performed with a whole-heart 230-μm spatial resolution CT scanner. *Radiology* 2017;**284**:676–84.
52. Pontone G, Andreini D, Petulla M, Annoni A, Guaricci AI, Innocenti E *et al.* Left atrium and pulmonary vein imaging using sub-millisiviert cardiac computed tomography: impact on radiofrequency catheter ablation cumulative radiation exposure and outcome in atrial fibrillation patients. *Int J Cardiol* 2017;**228**:805–11.
53. Romero J, Husain SA, Kelesidis I, Sanz J, Medina HM, Garcia MJ. Detection of left atrial appendage thrombus by cardiac computed tomography in patients with atrial fibrillation: a meta-analysis. *Circ Cardiovasc Imaging* 2013;**6**:185–94.
54. Wen Z, Zhang Z, Yu W, Fan Z, Du J, Lv B. Assessing the left atrial phasic volume and function with dual-source CT: comparison with 3T MRI. *Int J Cardiovasc Imaging* 2010; **26 Suppl 1**:83–92.
55. Fuchs A, Mejdahl MR, Kühl JT, Stisen ZR, Nilsson EJP, Køber LV *et al.* Normal values of left ventricular mass and cardiac chamber volumes assessed by 320-detector computed tomography angiography in the Copenhagen General Population Study. *Eur Heart J Cardiovasc Imaging* 2016;**17**:1009–17.
56. Di Biase L, Santangeli P, Anselmino M, Mohanty P, Salvetti I, Gili S *et al.* Does the left atrial appendage morphology correlate with the risk of stroke in patients with atrial fibrillation? Results from a multicenter study. *J Am Coll Cardiol* 2012;**60**:531–8.
57. Ling Z, McManigle J, Zipunnikov V, Pashakhanloo F, Khurram IM, Zimmerman SL *et al.* The association of left atrial low-voltage regions on electroanatomic mapping with low attenuation regions on cardiac computed tomography perfusion imaging in patients with atrial fibrillation. *Heart Rhythm* 2015;**12**:857–64.
58. Scully PR, Bastarrika G, Moon JC, Treibel TA. Myocardial extracellular volume quantification by cardiovascular magnetic resonance and computed tomography. *Curr Cardiol Rep* 2018;**20**:15.
59. Wong CX, Ganesan AN, Selvanayagam JB. Epicardial fat and atrial fibrillation: current evidence, potential mechanisms, clinical implications, and future directions. *Eur Heart J* 2017;**38**:1294–302.
60. Ang R, Hunter RJ, Baker V, Richmond L, Dhinoja M, Sporton S *et al.* Pulmonary vein measurements on pre-procedural CT/MR imaging can predict difficult pulmonary vein isolation and phrenic nerve injury during cryoballoon ablation for paroxysmal atrial fibrillation. *Int J Cardiol* 2015;**195**:253–8.
61. Horton R, Di Biase L, Reddy V, Neuzil P, Mohanty P, Sanchez J *et al.* Locating the right phrenic nerve by imaging the right pericardiophrenic artery with computerized tomographic angiography: implications for balloon-based procedures. *Heart Rhythm* 2010;**7**: 937–41.
62. Szilveszter B, Nagy AI, Vattay B, Apor A, Kolossváry M, Bartykowszki A *et al.* Left ventricular and atrial strain imaging with cardiac computed tomography: validation against echocardiography. *J Cardiovasc Comput Tomogr* 2020;**14**:363–9.
63. Niemelä M, Uusitalo V, Pöyhönen P, Schildt J, Lehtonen J, Kupari M. Incidence and predictors of atrial fibrillation in cardiac sarcoidosis: a multimodality imaging study. *JACC Cardiovasc Imaging* 2022;**15**:1622–31.
64. Watanabe E, Miyagawa M, Uetani T, Kinoshita M, Kitazawa R, Kurata M *et al.* Positron emission tomography/computed tomography detection of increased 18F-fluorodeoxyglucose uptake in the cardiac atria of patients with atrial fibrillation. *Int J Cardiol* 2019;**283**:171–7.
65. Li L, Gao J, Chen B-X, Liu X, Shi L, Wang Y *et al.* Fibroblast activation protein imaging in atrial fibrillation: a proof-of-concept study. *J Nucl Cardiol* 2023;**30**:2712–20.
66. Kupusovic J, Kessler L, Bruns F, Bohnen J-E, Nekolla SG, Weber MM *et al.* Visualization of fibroblast activation using 68Ga-FAPI PET/CT after pulmonary vein isolation with pulsed field compared with cryoballoon ablation. *J Nucl Cardiol* 2023;**30**:2018–28.
67. McDonagh TA, Metra M, Adamo M, Gardner RS, Baumbach A, Böhm M *et al.* ESC guidelines for the diagnosis and treatment of acute and chronic heart failure. *Eur Heart J* 2021;**42**:3599–726.
68. Gupta S, Matulevicius SA, Ayers CR, Berry JD, Patel PC, Markham DW *et al.* Left atrial structure and function and clinical outcomes in the general population. *Eur Heart J* 2013;**34**:278–85.
69. Habibi M, Chahal H, Opdahl A, Gjesdal O, Helle-Valle TM, Heckbert SR *et al.* Association of CMR-measured LA function with heart failure development: results from the MESA study. *JACC Cardiovasc Imaging* 2014;**7**:570–9.
70. Nagueh SF, Smiseth OA, Appleton CP, Byrd BF, Dokainish H, Edvardsen T *et al.* Recommendations for the evaluation of left ventricular diastolic function by echocardiography: an update from the American Society of Echocardiography and the European Association of Cardiovascular Imaging. *Eur Heart J Cardiovasc Imaging* 2016;**17**:1321–60.
71. Thomas L, Marwick TH, Popescu BA, Donal E, Badano LP. Left atrial structure and function, and left ventricular diastolic dysfunction: JACC state-of-the-art review. *J Am Coll Cardiol* 2019;**73**:1961–77.
72. Letnes JM, Nes B, Vaardal-Lunde K, Slette MB, Mølmen-Hansen HE, Aspenes ST *et al.* Left atrial volume, cardiorespiratory fitness, and diastolic function in healthy individuals: the HUNT study, Norway. *J Am Heart Assoc* 2020;**9**:e014682.
73. Morris DA, Belyavskiy E, Aravind-Kumar R, Kropf M, Frydas A, Braunauer K *et al.* Potential usefulness and clinical relevance of adding left atrial strain to left atrial volume index in the detection of left ventricular diastolic dysfunction. *JACC Cardiovasc Imaging* 2018;**11**:1405–15.
74. Singh A, Addetia K, Maffessanti F, Mor-Avi V, Lang RM. LA strain for categorization of LV diastolic dysfunction. *JACC Cardiovasc Imaging* 2017;**10**:735–43.
75. Smiseth OA, Morris DA, Cardim N, Cikes M, Delgado V, Donal E *et al.* Multimodality imaging in patients with heart failure and preserved ejection fraction: an expert consensus document of the European Association of Cardiovascular Imaging. *Eur Heart J Cardiovasc Imaging* 2022;**23**:e34–61.
76. Morris DA, Takeuchi M, Krisper M, Köhncke C, Bekfani T, Carstensen T *et al.* Normal values and clinical relevance of left atrial myocardial function analysed by speckle-tracking echocardiography: multicentre study. *Eur Heart J Cardiovasc Imaging* 2015; **16**:364–72.
77. Inoue K, Khan FH, Remme EW, Ohte N, García-Izquierdo E, Chetrit M *et al.* Determinants of left atrial reservoir and pump strain and use of atrial strain for evaluation of left ventricular filling pressure. *Eur Heart J Cardiovasc Imaging* 2021;**23**:61–70.
78. Santos ABS, Kraigher-Krainer E, Gupta DK, Claggett B, Zile MR, Pieske B *et al.* Impaired left atrial function in heart failure with preserved ejection fraction. *Eur J Heart Fail* 2014; **16**:1096–103.
79. Santos ABS, Roca GQ, Claggett B, Sweitzer NK, Shah SJ, Anand IS *et al.* Prognostic relevance of left atrial dysfunction in heart failure with preserved ejection fraction. *Circ Heart Fail* 2016;**9**:e002763.
80. Kramer DG, Trikalinos TA, Kent DM, Antonopoulos GV, Konstam MA, Udelson JE. Quantitative evaluation of drug or device effects on ventricular remodeling as predictors of therapeutic effects on mortality in patients with heart failure and reduced ejection fraction: a meta-analytic approach. *J Am Coll Cardiol* 2010;**56**:392–406.
81. Cameli M, Lisi M, Mondillo S, Padeletti M, Ballo P, Tsioulpas C *et al.* Left atrial longitudinal strain by speckle tracking echocardiography correlates well with left ventricular filling pressures in patients with heart failure. *Cardiovasc Ultrasound* 2010;**8**:14.
82. McDonagh TA, Metra M, Adamo M, Gardner RS, Baumbach A, Böhm M *et al.* 2021 ESC guidelines for the diagnosis and treatment of acute and chronic heart failure. *Eur Heart J* 2021;**42**:3599–726.
83. Welles CC, Ku IA, Kwan DM, Whooley MA, Schiller NB, Turakhia MP. Left atrial function predicts heart failure hospitalization in subjects with preserved ejection fraction and coronary heart disease: longitudinal data from the Heart and Soul Study. *J Am Coll Cardiol* 2012;**59**:673–80.
84. Lønborg JT, Engstrøm T, Møller JE, Ahtarovski KA, Kelbæk H, Holmvang L *et al.* Left atrial volume and function in patients following ST elevation myocardial infarction and the association with clinical outcome: a cardiovascular magnetic resonance study. *Eur Heart J Cardiovasc Imaging* 2013;**14**:118–27.
85. Gerber BL, Castilho B. The importance of left atrial function in ischemic cardiomyopathy. *JACC Adv* 2024;**3**:100791.
86. Ersbøll M, Andersen MJ, Valeur N, Mogensen UM, Waziri H, Møller JE *et al.* The prognostic value of left atrial peak reservoir strain in acute myocardial infarction is dependent on left ventricular longitudinal function and left atrial size. *Circ Cardiovasc Imaging* 2013;**6**:26–33.
87. Antoni ML, ten Brinke EA, Atary JZ, Marsan NA, Holman ER, Schalij MJ *et al.* Left atrial strain is related to adverse events in patients after acute myocardial infarction treated with primary percutaneous coronary intervention. *Heart* 2011;**97**:1332–7.
88. Schuster A, Backhaus SJ, Stiermaier T, Navarra J-L, Uhlig J, Rommel K-P *et al.* Left atrial function with MRI enables prediction of cardiovascular events after myocardial infarction: insights from the AIDA STEMI and TATORT NSTEMI trials. *Radiology* 2019;**293**: 292–302.
89. Beinart R, Boyko V, Schwammenthal E, Kuperstein R, Sagie A, Hod H *et al.* Long-term prognostic significance of left atrial volume in acute myocardial infarction. *J Am Coll Cardiol* 2004;**44**:327–34.
90. Møller JE, Hillis GS, Oh JK, Seward JB, Reeder GS, Wright RS *et al.* Left atrial volume: a powerful predictor of survival after acute myocardial infarction. *Circulation* 2003;**107**: 2207–12.
91. Vieira MJ, Teixeira R, Gonçalves L, Gersh BJ. Left atrial mechanics: echocardiographic assessment and clinical implications. *J Am Soc Echocardiogr* 2014;**27**:463–78.
92. Cuspidi C, Sala C, Tadic M, Baccanelli G, Gherbesi E, Grassi G *et al.* Left atrial volume in elite athletes: a meta-analysis of echocardiographic studies. *Scand J Med Sci Sports* 2019; **29**:922–32.
93. D'Ascenzi F, Pelliccia A, Natali BM, Cameli M, Lisi M, Focardi M *et al.* Training-induced dynamic changes in left atrial reservoir, conduit, and active volumes in professional soccer players. *Eur J Appl Physiol* 2015;**115**:1715–23.
94. Spencer L, Wright L, Foulkes SJ, Rowe SJ, Dillon HT, Climie R *et al.* Characterizing the influence of cardiorespiratory fitness on left atrial size and function in the general population. *Am J Physiol Heart Circ Physiol* 2024;**326**:H1269–78.
95. Iskandar A, Mujtaba MT, Thompson PD. Left atrium size in elite athletes. *JACC Cardiovasc Imaging* 2015;**8**:753–62.
96. D'Ascenzi F, Pelliccia A, Natali BM, Cameli M, Andrei V, Incampo E *et al.* Increased left atrial size is associated with reduced atrial stiffness and preserved reservoir function in athlete's heart. *Int J Cardiovasc Imaging* 2015;**31**:699–705.

97. Luthi P, Zuber M, Ritter M, Oechslin EN, Jenni R, Seifert B *et al.* Echocardiographic findings in former professional cyclists after long-term deconditioning of more than 30 years. *Eur J Echocardiogr* 2008;**9**:261–7.
98. D'Andrea A, Riegler L, Cocchia R, Scarafile R, Salerno G, Gravino R *et al.* Left atrial volume index in highly trained athletes. *Am Heart J* 2010;**159**:1155–61.
99. Sanz-de la Garza M, Grazioli G, Bijnens BH, Sarvari SI, Guasch E, Pajuelo C *et al.* Acute, exercise dose-dependent impairment in atrial performance during an endurance race: 2D ultrasound speckle-tracking strain analysis. *JACC Cardiovasc Imaging* 2016;**9**:1380–8.
100. Schnell F, Claessen G, La Gerche A, Claus P, Bogaert J, Delcroix M *et al.* Atrial volume and function during exercise in health and disease. *J Cardiovasc Magn Reson* 2017;**19**:104.
101. Gabrielli L, Bijnens BH, Brambila C, Duchateau N, Marin J, Sitges-Serra I *et al.* Differential atrial performance at rest and exercise in athletes: potential trigger for developing atrial dysfunction? *Scand J Med Sci Sports* 2016;**26**:1444–54.
102. La Gerche A, Claessen G. Increased flow, dam walls, and upstream pressure: the physiological challenges and atrial consequences of intense exercise. *JACC Cardiovasc Imaging* 2016;**9**:1389–91.
103. Sørensen E, Myrstad M, Solberg MG, Øie E, Tveit A, Aarønæs M. Left atrial function in male veteran endurance athletes with paroxysmal atrial fibrillation. *Eur Heart J Cardiovasc Imaging* 2021;**23**:137–46.
104. Trivedi SJ, Claessen G, Stefani L, Flannery MD, Brown P, Janssens K *et al.* Differing mechanisms of atrial fibrillation in athletes and non-athletes: alterations in atrial structure and function. *Eur Heart J Cardiovasc Imaging* 2020;**21**:1374–83.
105. Hubert A, Galand V, Donal E, Pavin D, Galli E, Martins RP *et al.* Atrial function is altered in lone paroxysmal atrial fibrillation in male endurance veteran athletes. *Eur Heart J Cardiovasc Imaging* 2018;**19**:145–53.
106. Farhad H, Seidelmann SB, Vigneault D, Abbasi SA, Yang E, Day SM *et al.* Left atrial structure and function in hypertrophic cardiomyopathy sarcomere mutation carriers with and without left ventricular hypertrophy. *J Cardiovasc Magn Reson* 2017;**19**:107.
107. Siontis KC, Geske JB, Ong K, Nishimura RA, Ommen SR, Gersh BJ. Atrial fibrillation in hypertrophic cardiomyopathy: prevalence, clinical correlations, and mortality in a large high-risk population. *J Am Heart Assoc* 2014;**3**:e001002.
108. Maron BJ, Haas TS, Maron MS, Lesser JR, Browning JA, Chan RH *et al.* Left atrial remodeling in hypertrophic cardiomyopathy and susceptibility markers for atrial fibrillation identified by cardiovascular magnetic resonance. *Am J Cardiol* 2014;**113**:1394–400.
109. Debonnaire P, Joyce E, Hiemstra Y, Mertens BJ, Atsma DE, Schalij MJ *et al.* Left atrial size and function in hypertrophic cardiomyopathy patients and risk of new-onset atrial fibrillation. *Circ Arrhythm Electrophysiol* 2017;**10**:e004052.
110. Sivalokanathan S, Zghaib T, Greenland GV, Vasquez N, Kudchadkar SM, Kontari E *et al.* Hypertrophic cardiomyopathy patients with paroxysmal atrial fibrillation have a high burden of left atrial fibrosis by cardiac magnetic resonance imaging. *JACC Clin Electrophysiol* 2019;**5**:364–75.
111. Essayagh B, Resseguier N, Michel N, Casalta A-C, Renard S, Donghi V *et al.* Left atrial dysfunction as marker of poor outcome in patients with hypertrophic cardiomyopathy. *Arch Cardiovasc Dis* 2021;**114**:96–104.
112. Yang W-I, Shim CY, Kim YJ, Kim S-A, Rhee SJ, Choi E-Y *et al.* Left atrial volume index: a predictor of adverse outcome in patients with hypertrophic cardiomyopathy. *J Am Soc Echocardiogr* 2009;**22**:1338–43.
113. O'Mahony C, Jichi F, Pavlou M, Monserrat L, Anastasakis A, Rapezzi C *et al.* A novel clinical risk prediction model for sudden cardiac death in hypertrophic cardiomyopathy (HCM risk-SCD). *Eur Heart J* 2014;**35**:2010–20.
114. Hegde SM, Lester SJ, Solomon SD, Michels M, Elliott PM, Nagueh SF *et al.* Effect of Mavacamten on echocardiographic features in symptomatic patients with obstructive hypertrophic cardiomyopathy. *J Am Coll Cardiol* 2021;**78**:2518–32.
115. Pelliccia A, Borrazzo C, Caselli S, Lemme E, Musumeci MB, Maestrini V *et al.* Neither athletic training nor detraining affects LV hypertrophy in adult, low-risk patients with HCM. *JACC Cardiovasc Imaging* 2022;**15**:170–1.
116. Bandera F, Martone R, Chacko L, Ganesananthan S, Gilbertson JA, Ponticos M *et al.* Clinical importance of left atrial infiltration in cardiac transthyretin amyloidosis. *JACC Cardiovasc Imaging* 2022;**15**:17–29.
117. Aimo A, Fabiani I, Giannoni A, Mandoli GE, Pastore MC, Vergaro G *et al.* Multi-chamber speckle tracking imaging and diagnostic value of left atrial strain in cardiac amyloidosis. *Eur Heart J Cardiovasc Imaging* 2022;**24**:130–41.
118. Akintoye E, Majid M, Klein AL, Hanna M. Prognostic utility of left atrial strain to predict thrombotic events and mortality in amyloid cardiomyopathy. *JACC Cardiovasc Imaging* 2023;**16**:1371–83.
119. Mohty D, Boulogne C, Magne J, Varroud-Vial N, Martin S, Ettaif H *et al.* Prognostic value of left atrial function in systemic light-chain amyloidosis: a cardiac magnetic resonance study. *Eur Heart J Cardiovasc Imaging* 2016;**17**:961–9.
120. Tan Z, Yang Y, Wu X, Li S, Li L, Zhong L *et al.* Left atrial remodeling and the prognostic value of feature tracking derived left atrial strain in patients with light-chain amyloidosis: a cardiovascular magnetic resonance study. *Int J Cardiovasc Imaging* 2022;**38**:1519–32.
121. Kwong RY, Heydari B, Abbasi S, Steel K, Al-Mallah M, Wu H *et al.* Characterization of cardiac amyloidosis by atrial late gadolinium enhancement using contrast-enhanced cardiac magnetic resonance imaging and correlation with left atrial conduit and contractile function. *Am J Cardiol* 2015;**116**:622–9.
122. Huntjens PR, Zhang KW, Soyama Y, Karmpalioti M, Lenihan DJ, Gorcsan J. Prognostic utility of echocardiographic atrial and ventricular strain imaging in patients with cardiac amyloidosis. *JACC Cardiovasc Imaging* 2021;**14**:1508–19.
123. Vahanian A, Beyersdorf F, Praz F, Milojevic M, Baldus S, Bauersachs J *et al.* 2021 ESC/EACTS guidelines for the management of valvular heart disease. *Eur Heart J* 2022;**43**:561–632.
124. Otto CM, Nishimura RA, Bonow RO, Carabello BA, Erwin JP, Gentile F *et al.* 2020 ACC/AHA guideline for the management of patients with valvular heart disease: a report of the American College of Cardiology/American Heart Association Joint Committee on clinical practice guidelines. *Circulation* 2021;**143**:e72–227.
125. Essayagh B, Antoine C, Benfari G, Messika-Zeitoun D, Michelena H, Le Tourneau T *et al.* Prognostic implications of left atrial enlargement in degenerative mitral regurgitation. *J Am Coll Cardiol* 2019;**74**:858–70.
126. Cameli M, Pastore MC, Righini FM, Mandoli GE, D'Ascenzi F, Lisi M *et al.* Prognostic value of left atrial strain in patients with moderate asymptomatic mitral regurgitation. *Int J Cardiovasc Imaging* 2019;**35**:1597–604.
127. Stassen J, Namazi F, van der Bijl P, van Wijngaarden SE, Kamperidis V, Marsan NA *et al.* Left atrial reservoir function and outcomes in secondary mitral regurgitation. *J Am Soc Echocardiogr* 2022;**35**:477–85.e3.
128. Cameli M, Lisi M, Righini FM, Massoni A, Natali BM, Focardi M *et al.* Usefulness of atrial deformation analysis to predict left atrial fibrosis and endocardial thickness in patients undergoing mitral valve operations for severe mitral regurgitation secondary to mitral valve prolapse. *Am J Cardiol* 2013;**111**:595–601.
129. Zoghbi WA, Levine RA, Flachskampf F, Grayburn P, Gillam L, Leipsic J *et al.* Atrial functional mitral regurgitation: a JACC: cardiovascular imaging expert panel viewpoint. *JACC Cardiovasc Imaging* 2022;**15**:1870–82.
130. Stassen J, van Wijngaarden AL, Wu HW, Palmen M, Tomsic A, Delgado V *et al.* Left atrial remodeling after mitral valve repair for primary mitral regurgitation: evolution over time and prognostic significance. *J Cardiovasc Dev Dis* 2022;**9**:230.
131. Tastet L, Lim LJ, Bibby D, Hu G, Cristin L, Rich AH *et al.* Primary atriopathy in mitral valve prolapse: echocardiographic evidence and clinical implications. *Circ Cardiovasc Imaging* 2024;**17**:e016319.
132. Silbiger JJ. Advances in rheumatic mitral stenosis: echocardiographic, pathophysiologic, and hemodynamic considerations. *J Am Soc Echocardiogr* 2021;**34**:709–22.e1.
133. Candan O, Ozdemir N, Aung SM, Hatipoglu S, Karabay CY, Guler A *et al.* Atrial longitudinal strain parameters predict left atrial reverse remodeling after mitral valve surgery: a speckle tracking echocardiography study. *Int J Cardiovasc Imaging* 2014;**30**:1049–56.
134. Chien C-Y, Chen C-W, Lin T-K, Lin Y, Lin J-W, Li Y-D *et al.* Atrial deformation correlated with functional capacity in mitral stenosis patients. *Echocardiography* 2018;**35**:190–5.
135. Stassen J, Butcher SC, Namazi F, Ajmone Marsan N, Bax JJ, Delgado V. Left atrial deformation imaging and atrial fibrillation in patients with rheumatic mitral stenosis. *J Am Soc Echocardiogr* 2022;**35**:486–94.e2.
136. Meng Q-L, Meng H, Tao J, Yang S, Wang H. The role of left atrial strain in patients with functional tricuspid regurgitation before and after annuloplasty: a long-term follow-up study. *Cardiovasc Ultrasound* 2021;**19**:33.
137. Bouchahda N, Kallala MY, Zemni I, Ben Messaoud M, Boussaada M, Hasnaoui T *et al.* Left atrium reservoir function is central in patients with rheumatic mitral stenosis. *Int J Cardiovasc Imaging* 2021;**38**:1257–66.
138. Ancona R, Comenale Pinto S, Caso P, Di Salvo G, Severino S, D'Andrea A *et al.* Two-dimensional atrial systolic strain imaging predicts atrial fibrillation at 4-year follow-up in asymptomatic rheumatic mitral stenosis. *J Am Soc Echocardiogr* 2013;**26**:270–7.
139. Caso P, Ancona R, Di Salvo G, Comenale Pinto S, Macrino M, Di Palma V *et al.* Atrial reservoir function by strain rate imaging in asymptomatic mitral stenosis: prognostic value at 3 year follow-up. *Eur J Echocardiogr* 2009;**10**:753–9.
140. Mahfouz RA, Gouda M, Abdelhamed M. Relation between left atrial strain and exercise tolerance in patients with mild mitral stenosis: an insight from 2D speckle-tracking echocardiography. *Echocardiography* 2020;**37**:1406–12.
141. Samrat S, Sofi NU, Aggarwal P, Sinha SK, Pandey U, Sharma AK *et al.* Assessment of the left atrial reservoir function and left atrial volume after percutaneous balloon mitral valvuloplasty using peak atrial longitudinal strain. *Cureus* 2022;**14**:e22395.
142. Athayde GRS, Nascimento BR, Elmariah S, Lodi-Junqueira L, Soares JR, Saad GP *et al.* Impact of left atrial compliance improvement on functional status after percutaneous mitral valvuloplasty. *Catheter Cardiovasc Interv* 2019;**93**:156–63.
143. Ansari B, Siddiqui S, Barge V, Dash PK. Study of immediate and late effects of successful PTMC on left atrial appendage function in patients with severe rheumatic mitral stenosis in sinus rhythm. *Indian Heart J* 2020;**72**:179–83.
144. Cameli M, Mandoli GE, Loiacono F, Sparla S, Iardino E, Mondillo S. Left atrial strain: a useful index in atrial fibrillation. *Int J Cardiol* 2016;**220**:208–13.
145. Nattel S, Burstein B, Dobrev D. Atrial remodeling and atrial fibrillation: mechanisms and implications. *Circ Arrhythm Electrophysiol* 2008;**1**:62–73.

146. Fatema K, Barnes ME, Bailey KR, Abhayaratna WP, Cha S, Seward JB *et al.* Minimum vs. maximum left atrial volume for prediction of first atrial fibrillation or flutter in an elderly cohort: a prospective study. *Eur J Echocardiogr* 2009;**10**:282–6.
147. Njoku A, Kannabhiran M, Arora R, Reddy P, Gopinathannair R, Lakkireddy D *et al.* Left atrial volume predicts atrial fibrillation recurrence after radiofrequency ablation: a meta-analysis. *Europace* 2018;**20**:33–42.
148. Chiotis S, Doundoulakis I, Pagkalidou E, Piperis C, Zafeiropoulos S, Botis M *et al.* Total atrial conduction time as a predictor of atrial fibrillation recurrence: a systematic review and meta-analysis. *Cardiol Rev* 2023;**33**:70–6.
149. Pastore MC, De Carli G, Mandoli GE, D'Ascenzi F, Focardi M, Contorni F *et al.* The prognostic role of speckle tracking echocardiography in clinical practice: evidence and reference values from the literature. *Heart Fail Rev* 2021;**26**:1371–81.
150. Petre I, Onciul S, Iancovici S, Zamfir D, Stoian M, Scărlătescu A *et al.* Left atrial strain for predicting atrial fibrillation onset in hypertensive patients. *High Blood Press Cardiovasc Prev* 2019;**26**:331–7.
151. Sade LE, Keskin S, Can U, Çolak A, Yüce D, Çiftçi O *et al.* Left atrial mechanics for secondary prevention from embolic stroke of undetermined source. *Eur Heart J Cardiovasc Imaging* 2022;**23**:381–91.
152. Cameli M, Lisi M, Reccia R, Bennati E, Malandrino A, Solari M *et al.* Pre-operative left atrial strain predicts post-operative atrial fibrillation in patients undergoing aortic valve replacement for aortic stenosis. *Int J Cardiovasc Imaging* 2014;**30**:279–86.
153. Pathan F, Sivaraj E, Negishi K, Rafiudeen R, Pathan S, D'Elia N *et al.* Use of atrial strain to predict atrial fibrillation after cerebral ischemia. *JACC Cardiovasc Imaging* 2018;**11**:1557–65.
154. Shaikh AY, Maan A, Khan UA, Aurigemma GP, Hill JC, Kane JL *et al.* Speckle echocardiographic left atrial strain and stiffness index as predictors of maintenance of sinus rhythm after cardioversion for atrial fibrillation: a prospective study. *Cardiovasc Ultrasound* 2012;**10**:48.
155. Tops LF, Delgado V, Bertini M, Marsan NA, Den Uijl DW, Trines SAIP *et al.* Left atrial strain predicts reverse remodeling after catheter ablation for atrial fibrillation. *J Am Coll Cardiol* 2011;**57**:324–31.
156. Ma X-X, Boldt L-H, Zhang Y-L, Zhu M-R, Hu B, Parwani A *et al.* Clinical relevance of left atrial strain to predict recurrence of atrial fibrillation after catheter ablation: a meta-analysis. *Echocardiography* 2016;**33**:724–33.
157. Kuppahally SS, Akoum N, Burgon NS, Badger TJ, Kholmovski EG, Vijayakumar S *et al.* Left atrial strain and strain rate in patients with paroxysmal and persistent atrial fibrillation: relationship to left atrial structural remodeling detected by delayed-enhancement MRI. *Circ Cardiovasc Imaging* 2010;**3**:231–9.
158. Bos D, Vernooij MW, Shahzad R, Kavousi M, Hofman A, van Walsum T *et al.* Epicardial fat volume and the risk of atrial fibrillation in the general population free of cardiovascular disease. *JACC Cardiovasc Imaging* 2017;**10**:1405–7.
159. Wong CX, Sun MT, Odutayo A, Emdin CA, Mahajan R, Lau DH *et al.* Associations of epicardial, abdominal, and overall adiposity with atrial fibrillation. *Circ Arrhythm Electrophysiol* 2016;**9**:e004378.
160. Syed FF, DeSimone CV, Friedman PA, Asirvatham SJ. Left atrial appendage exclusion for atrial fibrillation. *Heart Fail Clin* 2016;**12**:273–97.
161. Quintana RA, Dong T, Vajapey R, Reyaldeen R, Kwon DH, Harb S *et al.* Intra- and post-procedural multimodality imaging in atrial fibrillation. *Circ Cardiovasc Imaging* 2022;**15**:e014804.
162. Manning WJ, Weintraub RM, Waksmonski CA, Haering JM, Rooney PS, Maslow AD *et al.* Accuracy of transesophageal echocardiography for identifying left atrial thrombi. A prospective, intraoperative study. *Ann Intern Med* 1995;**123**:817–22.
163. Jung PH, Mueller M, Schuhmann C, Eickhoff M, Schneider P, Seemueller G *et al.* Contrast enhanced transesophageal echocardiography in patients with atrial fibrillation referred to electrical cardioversion improves atrial thrombus detection and may reduce associated thromboembolic events. *Cardiovasc Ultrasound* 2013;**11**:1.
164. Yaghi S, Liberman AL, Atalay M, Song C, Furie KL, Kamel H *et al.* Cardiac magnetic resonance imaging: a new tool to identify cardioaortic sources in ischaemic stroke. *J Neurol Neurosurg Psychiatry* 2017;**88**:31–7.
165. Kwong Y, Troupis J. Cardiac CT imaging in the context of left atrial appendage occlusion. *J Cardiovasc Comput Tomogr* 2015;**9**:13–8.
166. Hur J, Kim YJ, Lee H-J, Nam JE, Hong YJ, Kim HY *et al.* Cardioembolic stroke: dual-energy cardiac CT for differentiation of left atrial appendage thrombus and circulatory stasis. *Radiology* 2012;**263**:688–95.
167. Teunissen C, Habets J, Velthuis BK, Cramer MJ, Loh P. Double-contrast, single-phase computed tomography angiography for ruling out left atrial appendage thrombus prior to atrial fibrillation ablation. *Int J Cardiovasc Imaging* 2017;**33**:121–8.
168. Hur J, Kim YJ, Lee H-J, Nam JE, Ha J-W, Heo JH *et al.* Dual-enhanced cardiac CT for detection of left atrial appendage thrombus in patients with stroke: a prospective comparison study with transesophageal echocardiography. *Stroke* 2011;**42**:2471–7.
169. Goldman ME, Pearce LA, Hart RG, Zabalgoitia M, Asinger RW, Safford R *et al.* Pathophysiologic correlates of thromboembolism in nonvalvular atrial fibrillation: I. Reduced flow velocity in the left atrial appendage (the Stroke Prevention in Atrial Fibrillation [SPAF-III] study). *J Am Soc Echocardiogr* 1999;**12**:1080–7.
170. Soulat-Dufour L, Lang S, Etienney A, Ederhy S, Ancedy Y, Adavane S *et al.* Correlation between left atrial spontaneous echocardiographic contrast and 5-year stroke/death in patients with non-valvular atrial fibrillation. *Arch Cardiovasc Dis* 2020;**113**:525–33.
171. Li Z, Liu Q, Liu F, Hidru TH, Tang Y, Cong T *et al.* Nomogram to predict left atrial thrombus or spontaneous echo contrast in patients with non-valvular atrial fibrillation. *Front Cardiovasc Med* 2021;**8**:737551.
172. Echocardiographic predictors of stroke in patients with atrial fibrillation: a prospective study of 1066 patients from 3 clinical trials. *Arch Intern Med* 1998;**158**:1316–20.
173. Donal E, Lip GYH, Galderisi M, Goette A, Shah D, Marwan M *et al.* EACVI/EHRA expert consensus document on the role of multi-modality imaging for the evaluation of patients with atrial fibrillation. *Eur Heart J Cardiovasc Imaging* 2016;**17**:355–83.
174. Lowe BS, Kusunose K, Motoki H, Varr B, Shrestha K, Whitman C *et al.* Prognostic significance of left atrial appendage 'sludge' in patients with atrial fibrillation: a new transesophageal echocardiographic thromboembolic risk factor. *J Am Soc Echocardiogr* 2014;**27**:1176–83.
175. Khan IA. Transient atrial mechanical dysfunction (stunning) after cardioversion of atrial fibrillation and flutter. *Am Heart J* 2002;**144**:11–22.
176. Handke M, Harloff A, Hetzel A, Olschewski M, Bode C, Geibel A. Left atrial appendage flow velocity as a quantitative surrogate parameter for thromboembolic risk: determinants and relationship to spontaneous echocontrast and thrombus formation--a transesophageal echocardiographic study in 500 patients with cerebral ischemia. *J Am Soc Echocardiogr* 2005;**18**:1366–72.
177. Quintana RA, Dong T, Vajapey R, Reyaldeen R, Kwon DH, Harb S *et al.* Preprocedural multimodality imaging in atrial fibrillation. *Circ Cardiovasc Imaging* 2022;**15**:e014386.
178. Burrell LD, Horne BD, Anderson JL, Muhlestein JB, Whisenant BK. Usefulness of left atrial appendage volume as a predictor of embolic stroke in patients with atrial fibrillation. *Am J Cardiol* 2013;**112**:1148–52.
179. Ayirala S, Kumar S, O'Sullivan DM, Silverman DI. Echocardiographic predictors of left atrial appendage thrombus formation. *J Am Soc Echocardiogr* 2011;**24**:499–505.
180. Doukky R, Khandelwal A, Garcia-Sayan E, Gage H. External validation of a novel transthoracic echocardiographic tool in predicting left atrial appendage thrombus formation in patients with nonvalvular atrial fibrillation. *Eur Heart J Cardiovasc Imaging* 2013;**14**:876–81.
181. Van Gelder IC, Rienstra M, Bunting KV, Casado-Arroyo R, Caso V, Crijns HJGM *et al.* Lumbers 2024 ESC guidelines for the management of atrial fibrillation developed in collaboration with the European Association for Cardio-Thoracic Surgery (EACTS). *Eur Heart J* 2024;**45**:3314–414.
182. Daoud EG, Glotzer TV, Wyse DG, Ezekowitz MD, Hilker C, Koehler J *et al.* Temporal relationship of atrial tachyarrhythmias, cerebrovascular events, and systemic emboli based on stored device data: a subgroup analysis of TRENDS. *Heart Rhythm* 2011;**8**:1416–23.
183. Sanna T, Diener H-C, Passman RS, Di Lazzaro V, Bernstein RA, Morillo CA *et al.* Cryptogenic stroke and underlying atrial fibrillation. *N Engl J Med* 2014;**370**:2478–86.
184. Al-Khatib SM, Allen LaPointe NM, Chatterjee R, Crowley MJ, Dupre ME, Kong DF *et al.* Rate- and rhythm-control therapies in patients with atrial fibrillation: a systematic review. *Ann Intern Med* 2014;**160**:760–73.
185. Overvad TF, Nielsen PB, Larsen TB, Søgaard P. Left atrial size and risk of stroke in patients in sinus rhythm. A systematic review. *Thromb Haemost* 2016;**116**:206–19.
186. Tsang TSM, Abhayaratna WP, Barnes ME, Miyasaka Y, Gersh BJ, Bailey KR *et al.* Prediction of cardiovascular outcomes with left atrial size: is volume superior to area or diameter? *J Am Coll Cardiol* 2006;**47**:1018–23.
187. Inoue YY, Alissa A, Khurram IM, Fukumoto K, Habibi M, Venkatesh BA *et al.* Quantitative tissue-tracking cardiac magnetic resonance (CMR) of left atrial deformation and the risk of stroke in patients with atrial fibrillation. *J Am Heart Assoc* 2015;**4**:e001844.
188. Clark A, Ferkh A, Vandenberg J, Elhindi J, Thomas L. Altered left atrial metrics in patients with cryptogenic stroke: a systematic review and meta-analysis. *Eur J Clin Invest* 2024;**54**:e14175.
189. Leong DP, Joyce E, Debonnaire P, Katsanos S, Holman ER, Schalij MJ *et al.* Left atrial dysfunction in the pathogenesis of cryptogenic stroke: novel insights from speckle-tracking echocardiography. *J Am Soc Echocardiogr* 2017;**30**:71–9.e1.
190. Kühnlein P, Mahnkopf C, Majersik JJ, Wilson BD, Mitlacher M, Tirschwell D *et al.* Atrial fibrosis in embolic stroke of undetermined source: a multicenter study. *Eur J Neurol* 2021;**28**:3634–9.
191. Tandon K, Tirschwell D, Longstreth WT, Smith B, Akoum N. Embolic stroke of undetermined source correlates to atrial fibrosis without atrial fibrillation. *Neurology* 2019;**93**:e381–7.
192. Kamel H, Soliman EZ, Heckbert SR, Kronmal RA, Longstreth WT, Nazarian S *et al.* P-wave morphology and the risk of incident ischemic stroke in the Multi-Ethnic Study of Atherosclerosis. *Stroke* 2014;**45**:2786–8.
193. Folsom AR, Nambi V, Bell EJ, Oluleye OW, Gottesman RF, Lutsey PL *et al.* Troponin T, N-terminal pro-B-type natriuretic peptide, and incidence of stroke: the atherosclerosis risk in communities study. *Stroke* 2013;**44**:961–7.
194. Russo C, Jin Z, Liu R, Iwata S, Tugcu A, Yoshita M *et al.* LA volumes and reservoir function are associated with subclinical cerebrovascular disease: the CABL (Cardiovascular Abnormalities and Brain Lesions) study. *JACC Cardiovasc Imaging* 2013;**6**:313–23.

195. Lip GYH, Nieuwlaat R, Pisters R, Lane DA, Crijns HJGM. Refining clinical risk stratification for predicting stroke and thromboembolism in atrial fibrillation using a novel risk factor-based approach: the euro heart survey on atrial fibrillation. *Chest* 2010;**137**:263–72.
196. Akoum N, Fernandez G, Wilson B, Mcgann C, Kholmovski E, Marrouche N. Association of atrial fibrosis quantified using LGE-MRI with atrial appendage thrombus and spontaneous contrast on transesophageal echocardiography in patients with atrial fibrillation. *J Cardiovasc Electrophysiol* 2013;**24**:1104–9.
197. Daccarett M, Badger TJ, Akoum N, Burgon NS, Mahnkopf C, Vergara G *et al.* Association of left atrial fibrosis detected by delayed-enhancement magnetic resonance imaging and the risk of stroke in patients with atrial fibrillation. *J Am Coll Cardiol* 2011;**57**:831–8.
198. Zhu M-R, Wang M, Ma X-X, Zheng D-Y, Zhang Y-L. The value of left atrial strain and strain rate in predicting left atrial appendage stasis in patients with nonvalvular atrial fibrillation. *Cardiol J* 2018;**25**:87–96.
199. Larsen BS, Aplin M, Høst N, Dominguez H, Christensen H, Christensen LM *et al.* Atrial cardiomyopathy in patients with ischaemic stroke: a cross-sectional and prospective cohort study-the COAST study. *BMJ Open* 2022;**12**:e061018.
200. Boyd A, Stoodley P, Richards D, Hui R, Harnett P, Vo K *et al.* Anthracyclines induce early changes in left ventricular systolic and diastolic function: a single centre study. *PLoS One* 2017;**12**:e0175544.
201. Piotrowski G, Gawor R, Bourge RC, Stasiak A, Potemski P, Gawor Z *et al.* Heart remodeling induced by adjuvant trastuzumab-containing chemotherapy for breast cancer overexpressing human epidermal growth factor receptor type 2: a prospective study. *Pharmacol Res* 2013;**78**:41–8.
202. Huang F, Brezden-Masley C, Chan KKW, Barfett JJ, Kirpalani A, Deva DP *et al.* Evaluation of left atrial remodeling using cardiovascular magnetic resonance imaging in breast cancer patients treated with adjuvant trastuzumab. *Eur Radiol* 2022;**32**:4234–42.
203. Timóteo AT, Moura Branco L, Filipe F, Galrinho A, Rio P, Portugal G *et al.* Cardiotoxicity in breast cancer treatment: what about left ventricular diastolic function and left atrial function? *Echocardiography* 2019;**36**:1806–13.
204. Moreno J, García-Sáez JA, Clavero M, Manganaro R, Moreno F, López J *et al.* Effect of breast cancer cardiotoxic drugs on left atrial myocardium mechanics. Searching for an early cardiotoxicity marker. *Int J Cardiol* 2016;**210**:32–4.
205. Bergamini C, Dolci G, Rossi A, Torelli F, Ghiselli L, Trevisani L *et al.* Left atrial volume in patients with HER2-positive breast cancer: one step further to predict trastuzumab-related cardiotoxicity. *Clin Cardiol* 2018;**41**:349–53.
206. Emerson P, Deshmukh T, Stefani L, Mahendran S, Hogg M, Brown P *et al.* Left atrial strain in cardiac surveillance of bone marrow transplant patients with prior anthracycline exposure. *Int J Cardiol* 2022;**354**:68–74.
207. Laufer-Perl M, Arias O, Dorfman SS, Baruch G, Rothschild E, Beer G *et al.* Left atrial strain changes in patients with breast cancer during anthracycline therapy. *Int J Cardiol* 2021;**330**:238–44.
208. Loar RW, Colquitt JL, Rainusso NC, Gramatges MM, Liu AM, Noel CV *et al.* Assessing the left atrium of childhood cancer survivors. *Int J Cardiovasc Imaging* 2021;**37**:155–62.
209. Shi J, Guo Y, Cheng L, Song F, Shu X. Early change in left atrial function in patients treated with anthracyclines assessed by real-time three-dimensional echocardiography. *Sci Rep* 2016;**6**:25512.
210. Menon D, Kadiu G, Sanil Y, Aggarwal S. Anthracycline treatment and left atrial function in children: a real-time 3-dimensional echocardiographic study. *Pediatr Cardiol* 2022;**43**:645–54.
211. Chen N, Liu A, Sun S, Wei H, Sun Q, Shang Z *et al.* Evaluation of left atrial function and mechanical dispersion in breast cancer patients after chemotherapy. *Clin Cardiol* 2022;**45**:540–8.
212. Ganatra S, Sharma A, Shah S, Chaudhry GM, Martin DT, Neilan TG *et al.* Ibrutinib-associated atrial fibrillation. *JACC Clin Electrophysiol* 2018;**4**:1491–500.
213. Singh A, El Hangouche N, McGee K, Gong F-F, Lentz R, Feinglass J *et al.* Utilizing left atrial strain to identify patients at risk for atrial fibrillation on ibrutinib. *Echocardiography* 2021;**38**:81–8.
214. Yu C, Negishi T, Thavendiranathan P, Pathan F, Marwick TH, Negishi K. Utility of baseline left atrial reservoir strain in predicting cardiotoxicity after chemotherapy: a SUCCOUR study subanalysis. *JACC Cardiovasc Imaging* 2024;**17**:708–9.
215. Park H, Kim KH, Kim HY, Cho JY, Yoon HJ, Hong YJ *et al.* Left atrial longitudinal strain as a predictor of cancer therapeutics-related cardiac dysfunction in patients with breast cancer. *Cardiovasc Ultrasound* 2020;**18**:28.
216. Deneke T, Kutyifa V, Hindricks G, Sommer P, Zeppenfeld K, Carbucicchio C *et al.* Pre- and post-procedural cardiac imaging (computed tomography and magnetic resonance imaging) in electrophysiology: a clinical consensus statement of the European Heart Rhythm Association and European Association of Cardiovascular Imaging of the European Society of Cardiology. *Europace* 2024;**26**:euae108.
217. Klein AL, Grimm RA, Murray RD, Apperson-Hansen C, Asinger RW, Black IW *et al.* Use of transesophageal echocardiography to guide cardioversion in patients with atrial fibrillation. *N Engl J Med* 2001;**344**:1411–20.
218. Klein AL, Jasper SE, Katz WE, Malouf JF, Pape LA, Stoddard MF *et al.* The use of enoxaparin compared with unfractionated heparin for short-term antithrombotic therapy in atrial fibrillation patients undergoing transoesophageal echocardiography-guided cardioversion: assessment of Cardioversion Using Transoesophageal Echocardiography (ACUTE) II randomized multicentre study. *Eur Heart J* 2006;**27**:2858–65.
219. Cappato R, Marchlinski FE, Hohnloser SH, Naccarelli GV, Xiang J, Wilber DJ *et al.* Uninterrupted rivaroxaban vs. uninterrupted vitamin K antagonists for catheter ablation in non-valvular atrial fibrillation. *Eur Heart J* 2015;**36**:1805–11.
220. Goette A, Merino JL, Ezekowitz MD, Zamoryakhin D, Melino M, Jin J *et al.* Edoxaban versus enoxaparin-warfarin in patients undergoing cardioversion of atrial fibrillation (ENSURE-AF): a randomised, open-label, phase 3b trial. *Lancet* 2016;**388**:1995–2003.
221. Ezekowitz MD, Pollack CV, Halperin JL, England RD, VanPelt Nguyen S, Spahr J *et al.* Apixaban compared to heparin/vitamin K antagonist in patients with atrial fibrillation scheduled for cardioversion: the EMANATE trial. *Eur Heart J* 2018;**39**:2959–71.
222. January CT, Wann LS, Calkins H, Chen LY, Cigarroa JE, Cleveland JC *et al.* 2019 AHA/ACC/HRS focused update of the 2014 AHA/ACC/HRS guideline for the management of patients with atrial fibrillation: a report of the American College of Cardiology/American Heart Association task force on clinical practice guidelines and the Heart Rhythm Society in Collaboration With the Society of Thoracic Surgeons. *Circulation* 2019;**140**:e125–51.
223. Black IW, Fatkin D, Sagar KB, Khandheria BK, Leung DY, Galloway JM *et al.* Exclusion of atrial thrombus by transesophageal echocardiography does not preclude embolism after cardioversion of atrial fibrillation. A multicenter study. *Circulation* 1994;**89**:2509–13.
224. Vincenti A, Genovesi S, Sonaglioni A, Binda G, Rigamonti E, Lombardo M *et al.* Mechanical atrial recovery after cardioversion in persistent atrial fibrillation evaluated by bidimensional speckle tracking echocardiography. *J Cardiovasc Med (Hagerstown)* 2019;**20**:745–51.
225. Tzeis S, Gerstenfeld EP, Kalman J, Saad E, Shamloo AS, Andrade JG. 2024 European Heart Rhythm Association/Heart Rhythm Society/Asia Pacific Heart Rhythm Society/Latin American Heart Rhythm Society expert consensus statement on catheter and surgical ablation of atrial fibrillation. *J Interv Card Electrophysiol* 2024;**67**:921–1072.
226. Mammadli A, Demirtola AI, Diker E. Impact of image integration on clinical and procedural outcomes of radiofrequency catheter ablation of atrial fibrillation: a meta-analysis of randomized controlled trials. *J Arrhythm* 2021;**37**:550–5.
227. Blandino A, Bianchi F, Grossi S, Biondi-Zoccai G, Conte MR, Gaido L *et al.* Left atrial substrate modification targeting low-voltage areas for catheter ablation of atrial fibrillation: a systematic review and meta-analysis. *Pacing Clin Electrophysiol* 2017;**40**:199–212.
228. Zghaib T, Keramati A, Chrispin J, Huang D, Balouch MA, Ciuffo L *et al.* Multimodal examination of atrial fibrillation substrate: correlation of left atrial bipolar voltage using multi-electrode fast automated mapping, point-by-point mapping, and magnetic resonance image intensity ratio. *JACC Clin Electrophysiol* 2018;**4**:59–68.
229. Calkins H, Hindricks G, Cappato R, Kim Y-H, Saad EB, Aguinaga L *et al.* HRS/EHRA/ECAS/APHRS/SOLAECE expert consensus statement on catheter and surgical ablation of atrial fibrillation. *Europace* 2018;**20**:e1–160.
230. Della Bella P, Fassini G, Cireddu M, Riva S, Carbucicchio C, Giraldi F *et al.* Image integration-guided catheter ablation of atrial fibrillation: a prospective randomized study. *J Cardiovasc Electrophysiol* 2009;**20**:258–65.
231. Caponi D, Corleto A, Scaglione M, Blandino A, Biasco L, Cristoforetti Y *et al.* Ablation of atrial fibrillation: does the addition of three-dimensional magnetic resonance imaging of the left atrium to electroanatomic mapping improve the clinical outcome? A randomized comparison of Carto-Merge vs. Carto-XP three-dimensional mapping ablation in patients with paroxysmal and persistent atrial fibrillation. *Europace* 2010;**12**:1098–104.
232. Marrouche NF, Wilber D, Hindricks G, Jais P, Akoum N, Marchlinski F *et al.* Association of atrial tissue fibrosis identified by delayed enhancement MRI and atrial fibrillation catheter ablation: the DECAAF study. *JAMA* 2014;**311**:498–506.
233. Jefairi NA, Camaioni C, Sridi S, Cheniti G, Takigawa M, Nivet H *et al.* Relationship between atrial scar on cardiac magnetic resonance and pulmonary vein reconnection after catheter ablation for paroxysmal atrial fibrillation. *J Cardiovasc Electrophysiol* 2019;**30**:727–40.
234. Rav Acha M, Tovia-Brodie O, Michowitz Y, Bayya F, Shaheen FF, Abuhatzera S *et al.* Cryoballoon-induced circumferential pulmonary vein fibrosis, assessed by late gadolinium-enhancement cardiac magnetic resonance imaging, and its correlation with clinical atrial fibrillation recurrence. *J Clin Med* 2023;**12**:2442.
235. Mansour M, Gerstenfeld EP, Patel C, Natale A, Whang W, Cuoco FA *et al.* Pulmonary vein narrowing after pulsed field versus thermal ablation. *Europace* 2024;**26**:euae038.
236. Vanhaverbeke M, Nuyens P, Bieliauskas G, Sondergaard L, Vejlstrup N, De Backer O. Facilitation techniques to cross the interatrial septum with intracardiac echocardiography during left atrial appendage closure. *Catheter Cardiovasc Interv* 2022;**100**:795–800.
237. Xu J, Gao Y, Liu C, Wang Y. Radiofrequency ablation for treatment of atrial fibrillation with the use of intracardiac echocardiography versus without intracardiac echocardiography: a meta-analysis of observational and randomized studies. *J Cardiovasc Electrophysiol* 2022;**33**:897–907.
238. Pimentel RC, Rahai N, Maccioni S, Khanna R. Differences in outcomes among patients with atrial fibrillation undergoing catheter ablation with versus without intracardiac echocardiography. *J Cardiovasc Electrophysiol* 2022;**33**:2015–47.

239. Gupta A, Perera T, Ganesan A, Sullivan T, Lau DH, Roberts-Thomson KC *et al.* Complications of catheter ablation of atrial fibrillation: a systematic review. *Circ Arrhythm Electrophysiol* 2013;**6**:1082–8.
240. Benali K, Khairy P, Hammache N, Petzl A, Da Costa A, Verma A *et al.* Procedure-related complications of catheter ablation for atrial fibrillation. *J Am Coll Cardiol* 2023;**8**:2089–99.
241. Katz ES, Tsiamtsiouris T, Applebaum RM, Schwartzbard A, Tunick PA, Kronzon I. Surgical left atrial appendage ligation is frequently incomplete: a transesophageal echocardiograhic study. *J Am Coll Cardiol* 2000;**36**:468–71.
242. Holmes DR, Kar S, Price MJ, Whisenant B, Sievert H, Doshi SK *et al.* Prospective randomized evaluation of the Watchman left atrial appendage closure device in patients with atrial fibrillation versus long-term warfarin therapy: the PREVAIL trial. *J Am Coll Cardiol* 2014;**64**:1–12.
243. Lakkireddy D, Thaler D, Ellis CR, Swarup V, Sondergaard L, Carroll J *et al.* Amplatzer amulet left atrial appendage occluder versus watchman device for stroke prophylaxis (amulet IDE): a randomized, controlled trial. *Circulation* 2021;**144**:1543–52.
244. Glikson M, Wolff R, Hindricks G, Mandrola J, Camm AJ, Lip GYH *et al.* EHRA/EAPCI expert consensus statement on catheter-based left atrial appendage occlusion—an update. *Europace* 2020;**22**:184.
245. Saw J, Holmes DR, Cavalcante JL, Freeman JV, Goldsweig AM, Kavinsky CJ *et al.* SCAI/HRS expert consensus statement on transcatheter left atrial appendage closure. *JACC Cardiovasc Interv* 2023;**16**:1384–400.
246. Fukutomi M, Fuchs A, Bieliauskas G, Wong I, Kofoed KF, Søndergaard L *et al.* Computed tomography-based selection of transseptal puncture site for percutaneous left atrial appendage closure. *EuroIntervention* 2022;**17**:e1435–44.
247. Afzal MR, Gabriels JK, Jackson GG, Chen L, Buck B, Campbell S *et al.* Temporal changes and clinical implications of delayed peridevice leak following left atrial appendage closure. *JACC Clin Electrophysiol* 2022;**8**:15–25.
248. Alkhouli M, Du C, Killu A, Simard T, Noseworthy PA, Friedman PA *et al.* Clinical impact of residual leaks following left atrial appendage occlusion: insights from the NCDR LAAO registry. *JACC Clin Electrophysiol* 2022;**8**:766–78.
249. Nielsen-Kudsk JE, Berti S, Caprioglio F, Ronco F, Arzamendi D, Betts T *et al.* Intracardiac echocardiography to guide Watchman FLX implantation: the ICE LAA study. *JACC Cardiovasc Interv* 2023;**16**:643–51.
250. Mill J, Harrison J, Saiz-Vivo M, Albors C, Morales X, Olivares AL *et al.* The role of the pulmonary veins on left atrial flow patterns and thrombus formation. *Sci Rep* 2024;**14**:5860.
251. Rusinaru D, Bohbot Y, Kowalski C, Ringle A, Maréchaux S, Tribouilloy C. Left atrial volume and mortality in patients with aortic stenosis. *J Am Heart Assoc* 2017;**6**:e006615.